RSC Advances

PAPER

View Article Online
View Journal | View Issue

Cite this: *RSC Adv.*, 2025, **15**, 39123

Reusing expired streptomycin and neomycin drugs as potential corrosion inhibitors for high brass alloys in NaCl solution: quantum, chemical, surface and electrochemical investigations

Ahmed Fawzy,*[a] Arafat Toghan,[b] Areej Al Bahir,[c] Emad M. Masoud,*[d] Magdi E. A. Zaki,[b] Minghua Huang,[e] Ahmed A. Farag[f] and H. S. Gadow[g]

Although drugs are essential for humans, they are perilous for the ecosystem when disposed of improperly. There are challenges in reusing them for other useful purposes, most notably as corrosion inhibitors; corrosion inhibition is an important industrial and economic aspect of protecting metals and the environment. Copper alloys are widely used in outdoor applications, especially in casting decorative items, but they have shortcomings in corrosion resistance. Herein, the ability of two expired drugs, streptomycin (I) and neomycin (II), to resist the corrosion of a high Cu–Zn alloy in a 3.5% NaCl environment was studied in detail *via* electrochemical, gravimetric and microscopic techniques as well as theoretical calculations. The electrochemical results showed that there was an increase in the corrosion rate of the examined alloy with increasing [NaCl]. The addition of 500 mg L^{-1} of the tested drugs strongly inhibited alloy corrosion, and the inhibition efficiencies (% IEs) reached 87.4% and 91.6% with drugs I and II, respectively. The obtained gravimetric outcomes indicated that the values of % IEs were augmented with increasing drug dosages, while they decreased as [NaCl] and solution temperature increased. The higher % IEs were attributed to the strong adsorption of the drugs on the brass surface. This adsorption was suggested to be physical and obeyed the Langmuir adsorption isotherm. Polarization assessments indicated that these drugs were mixed-type inhibitors with an anodic priority. All thermodynamic/kinetic parameters were determined through full adsorption assays, and the possible inhibition mechanism was proposed. Computational methods provided further support and clarification of the inhibition mechanism of these drugs. All results of the applied techniques were in excellent conformity with each other and with the employed computational methods.

Received 28th August 2025
Accepted 30th September 2025

DOI: 10.1039/d5ra06456b

rsc.li/rsc-advances

1. Introduction

The natural phenomenon of deterioration of metals and alloys, termed corrosion, is regarded as a serious challenge in all countries because of both economic and environmental concerns.[1,2] The prevention or control of this phenomenon requires the usage of effectual methods. The addition of corrosion inhibitors denotes an applicable strategy to protect the surfaces of metals from the aggressiveness of the surrounding medium.[3] These corrosion inhibitors function *via* their potent adsorption on the metallic surfaces, forming protective layers. The principal characteristic of these inhibitors is the existence of certain functional groups that contain N, S, P and O atoms or π-electrons, which facilitate their adsorption on the metallic surfaces.[4,5]

Copper alloys are extensively utilized for various significant industrial purposes.[6] Brasses are important and noteworthy copper-based alloys, especially with zinc in different proportions and copper in the highest proportion, to achieve different physical and chemical properties.[7] They are known for their technological properties and find various applications in the fields of mechanical engineering, medical and arts. However, there are certain factors that make brass alloys corrode in aggressive media, especially in chloride environments.[8–25] The supreme forms of brass corrosion are dezincification,[17–26] stress-corrosion cracking,[17,18] and pitting corrosion.[19–21] In chloride

[a]*Chemistry Department, Faculty of Science, Assiut University, Assiut 71516, Egypt. E-mail: ahmed.sayed3@science.aun.edu.eg*

[b]*Chemistry Department, College of Science, Imam Mohammad Ibn Saud Islamic University (IMSIU), Riyadh 11623, Saudi Arabia*

[c]*Chemistry Department, Faculty of Science, King Khalid University, Abha 64734, Saudi Arabia*

[d]*Department of Chemistry, Faculty of Science, Islamic University of Madinah, 42351 Madinah, Saudi Arabia. E-mail: emad.youssef@iu.edu.sa*

[e]*School of Materials Science and Engineering, Ocean University of China, Qingdao 266100, China*

[f]*Egyptian Petroleum Research Institute (EPRI), Nasr City, Cairo 11727, Egypt*

[g]*High Institute of Engineering and Technology, New Damietta 42519, Egypt*

media, dezincification occurs in the early stages of corrosion, in which zinc is anodically dissolved, leading to the appearance of vacancies on the alloy surface.[22,23] Also, in chloride media, multiple layers containing oxides of zinc and copper (ZnO, Cu_2O, and CuO) are constructed on the alloy surface, which passivate the alloy surface and inhibit its corrosion.[15,16,20,21] At relatively lower concentrations of Cl^- ions, a CuCl layer is formed, which slightly protects the alloy surface from corrosion attacks.[24,25] At critical [Cl^-], the rate of corrosion increases markedly because of the formation of soluble $CuCl_2^-$ complexes and the discontinuity of the passivation layer.[19] In the presence of Cl^- ions, dezincification and localized attacks on the alloy surface occur simultaneously.[7–9] It was reported[20,21] that brass alloys are much more disposed to pitting than copper, as the formed ZnO layer is less resistant to corrosion.

Due to their extensive utilization in diverse fields, the corrosion of brass alloys and their protection have attracted great consideration, and a lot of investigations have been made in this regard. Therefore, an immense number of organic compounds have been previously examined as inhibitors for brass alloy corrosion, especially in Cl^- media,[26–45] acidic media,[46–52] alkaline media[53,54] and other environments.[55–58] Benzotriazole derivatives are the most examined organic inhibitors for the corrosion of brass alloys in Cl^- media.[26–34] The higher efficiencies of benzotriazole derivatives are due to the formation of chemisorption compounds or multicomponent structures on the surfaces of brass alloys that, in addition to the oxides of copper and zinc, comprise polymer systems with Cu^+ and Zn^{2+} ions.[30–32] This leads to the construction of protective layers on the alloy surface and prevents further dissolution and subsequent dezincification and pitting attacks. Various organic compounds have been investigated for this purpose, such as aminotriazole[35] and thiadiazole derivatives[36] and quinoline derivatives based on D-glucose,[47] 4-fluorophenyl-2,5-dithiohydrazodicarbonamide,[38] 1,3-bis-diethylamino-propan-2-ol[39] and cysteine.[50] Early investigations were dedicated to the study of variamine blue B,[41] 2-mercaptobenzothiazole and Tween-80,[42] and self-assembled silane[43] as corrosion inhibitors for brasses in chloride media.

Recently, many studies[59–67] have been devoted to investigating green or ecofriendly corrosion inhibitors that do not have any effect on the ecosystem because most of the employed inhibitors are toxic and have highly harmful effects on the environment. Some pharmaceutical drugs contain, in their chemical structures, various electronegative functional groups, heteroatoms, π systems and/or heterocycles that give these drugs good adsorption capabilities on the metallic surfaces, leading to a shielding layer construction that protects the metal surfaces.[68–71] In addition, such drugs have good aqueous solubilities and abilities to form complexes with the metal ions released in the solution through the corrosion process.[70–74] Thus, these pharmaceuticals are considered as promising, sustainable, effectual, and safe[68–74] anticorrosive agents, instead of other highly toxic and hazardous inhibitors like arsenic, chromate, molybdate, and phosphate compounds.[75–77] Accordingly, expired pharmaceuticals are safely used as corrosion inhibitors to achieve economic and environmental benefits. To date, several drugs have been investigated and found to be effective in inhibiting the corrosion of many metals and alloys in different media.[68–74] Streptomycin and neomycin are two drugs from the aminoglycoside antibiotics family that are utilized to treat several bacterial infections.[78] Fig. 1 illustrates the structures of the two drugs, which contain various nitrogen and oxygen heteroatoms and heterocyclic rings that permit these compounds to intensely adsorb on the metal surfaces. Hence, these drugs, which are expired, can be used as efficient, ecofriendly, water-soluble, available and free-of-cost inhibitors for the prevention or reduction of metallic corrosion.

The current research aimed to examine the inhibitory characteristics of expired streptomycin and neomycin drugs in the corrosion of high brass alloys in 3.5% NaCl at fixed temperatures. This work was performed using various experimental and computational techniques. The experimental techniques were electrochemical measurements (open circuit potentials, OCP, and potentiodynamic polarization, PDP) and the gravimetric or weight loss (WL) method. Also, the surface morphologies of the alloy surfaces in the absence and presence of the expired drugs were photographed by scanning electron microscopy (SEM). The employed computational methods were density functional theory (DFT) calculations, molecular dynamics (MD) simulations, Mulliken atomic charges, Fukui indices and molecular electrostatic potential (MESP) analysis.

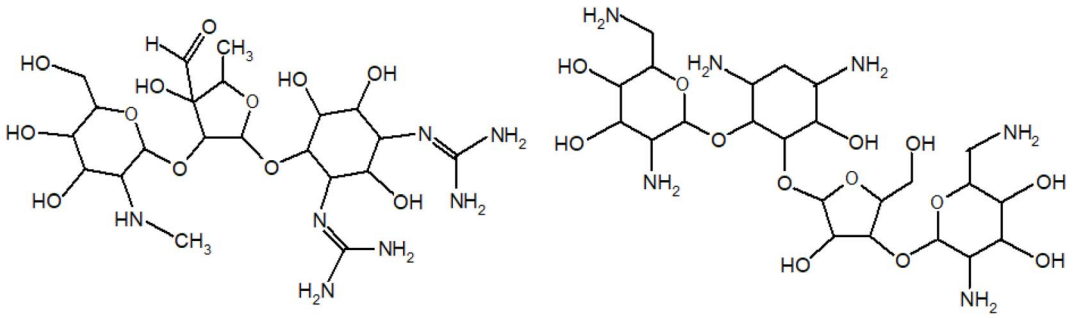

Streptomycin (I) **Neomycin (II)**

Fig. 1 Chemical structures of the tested drugs.

2. Experimental section

2.1 Materials

The examined alloy was the high brass alloy, Cu–35Zn (Central Metallurgical Research and Development Institute, Cairo, Egypt) with the chemical composition (wt%) of 35 Cu, 34.8 Zn, 0.15 Pb and 0.05 Sn. The sheets of the alloy were handled before each experiment by polishing using different SiC emery papers (200–1200), washing with bi-distilled water, degreasing with acetone, and lastly drying. Corrosion experiments were performed in a 3.5% NaCl (99.99%) blank solution without and with adding the expired drugs within the range from 100 to 500 mg L^{-1}. Solutions of the expired drugs, streptomycin sulfate (I) (Fluka, $C_{21}H_{39}N_7O_{12}\cdot H_2SO_4$, 679.70 g mol^{-1}, EXP 08-2024) and neomycin sulfate (II) (Fluka, $C_{23}H_{46}N_6O_{13}\cdot H_2SO_4$, 712.72 g mol^{-1}, EXP 06-2024) were prepared using bi-distilled water. Each experiment was performed about three times to attain consistent results and to check the reproducibility.

2.2 Methods

The techniques used in this investigation were experimental and computational. The experimental techniques were electrochemical measurements (OCP and PDP) and weight loss (WL) and surface analyses (SEM). The computational methods were DFT calculations, MD simulations, Mulliken atomic charges, Fukui indices and MESP analysis.

2.2.1 Experimental techniques

2.2.1.1 Electrochemical measurements. These measurements were carried out utilizing a temperature-controlled PGSTAT30 potentiostat–galvanostat in a three-electrode cell including a working electrode composed of the investigated brass alloy (Cu–35Zn) with an exposed surface area of 1.0 cm^2 (set in an epoxy resin), a saturated calomel electrode (SCE) as a reference electrode, and a Pt plate as a supplementary electrode. After treating the working electrode, it was immersed in the investigated solution at the OCP (or E_{OC}) for approximately 30 min or for a time till a fixed potential state was reached. PDP runs were scanned from −300 mV to +300 mV *versus* E_{corr} at a scan rate of 1.0 mV s^{-1}.

2.2.1.2 Weight loss (WL) measurements. In the WL measurements, the sheets of the brass alloy (~16.7 cm^2 area) were used. These sheets were treated as reported earlier[79,80] and submerged in 100 mL of the investigated solution for the time periods of 4 to 20 h in the temperature range from 288 K to 318 K. Then, the sheets were cleaned, dried, and weighed. The average losses in the weights of brass sheets (in mg cm^{-2}) were computed after each experiment.

2.2.1.3 Surface analysis. In the SEM study, a JEOL SEM at 5.0 kV was utilized. The surfaces of brass sheets were observed by SEM after immersion in the examined solution for about 24 h at 298 K.

2.2.2 Theoretical studies

2.2.2.1 DFT calculations. Using a DNP 4.4 basis set and a B3LYP functional, density functional theory (DFT) calculations were carried out using the Dmol3 module of the BIOVIA Materials Studio 2017 program. The goal of these computations was to reduce the chemical molecules' energies in a water environment. Additionally, in order to assess and compute a number of properties, including E_{HOMO}, E_{LUMO}, energy gap (ΔE), electronegativity (χ), hardness (η), global softness (σ), number of electrons transferred (N), energy of back-donation (E back-donation), and dipole moment (μ), the DFT calculations used the following equations:[81]

$$I, \text{(ionization potential)} = -E_{HOMO} \quad (1)$$

$$A, \text{(electron affinity)} = -E_{LUMO} \quad (2)$$

$$P_i = -\chi \quad (3)$$

$$P_i = (E_{LUMO} + E_{HOMO})/2 \quad (4)$$

$$\eta = \Delta E/2 = (E_{LUMO} - E_{HOMO})/2 \quad (5)$$

$$\sigma = 1/\eta \quad (6)$$

$$\omega, \text{(electrophilicty index)} = {P_i}^2/2\eta \quad (7)$$

$$\varepsilon, \text{(nucleophilicity index)} = 1/\omega \quad (8)$$

The work function of iron is represented in the equations by the symbol φ, while the inhibitor's electronegativity is shown by the symbol χ_{inh}. The chemical hardness of the inhibitor and iron (0 eV) are denoted by η_{Fe} and η_{inh}, respectively.

2.2.2.2 MD simulation. Furthermore, MD simulations were performed using the adsorption finder module in BIOVIA Materials Studio 2017 software to ascertain the optimal configurations of the two compounds' molecules to adsorb onto the Cu (111) surface.[82] The COMPASS force field was used to achieve the best possible results for the adsorbate molecules. Then, in a simulation box (37.24 Å × 37.24 Å × 59.81 Å), we discovered the adsorption of inhibitor molecules, chloride ions, hydronium ions, and water molecules onto the Cu (111) surface.[83] The Cu (111) surface was chosen for the adsorption simulation because previous research has shown it to be the most stable and prevalent facet, making up over 65% of the copper crystals' total surface area.[84]

2.2.2.3 Mulliken atomic charges and Fukui indices. The localization of donor and acceptor sites of the molecule's active centers can be elucidated through the application of Mulliken atomic charges and Fukui indices.

2.2.2.4 MESP. To accurately identify the pertinent chemical reactions, the molecular electrostatic potential (MESP) map was utilized. The electrostatic potential was visualized through a color gradient at various locations on the electron density surface.

3. Results and discussion

3.1 Electrochemical measurements

3.1.1 OCP measurements. The effect of the corrosive medium (NaCl) concentration on the value of E_{OC} of the examined brass alloy was investigated at 298 K, as shown in Fig. 2. It can be noticed that the OCP values became more positive and then almost stabilized within 20–30 min, indicating the formation of a stable passive layer on the electrode

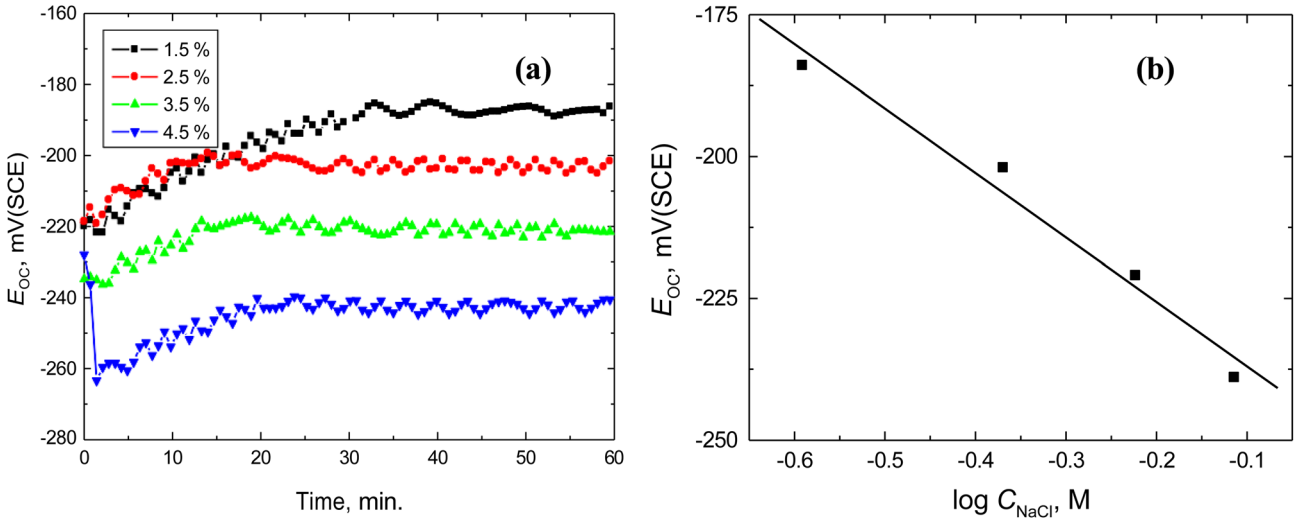

Fig. 2 Variation in the E_{OC} with time (a) and with NaCl concentration (b) during the corrosion of copper in sodium chloride solutions at 298 K.

surface,[85] *i.e.* a state of thermodynamic equilibrium (Fig. 2a). In contrast, as the NaCl concentration increased, the OCP shifted drastically to more negative values, indicating the acceleration of the cathodic reaction, *i.e.* weakening or dissolution of the passive film as a result of an increased corrosion rate.[86] Fig. 2b illustrates a linear relationship between E_{OC} and log[NaCl], agreeing with eqn (9):[86]

$$E_{OC} = a - b\log[\mathrm{NaCl}] \quad (9)$$

where a and b are constants related to the composition of the brass alloy, which are found to be −348 and −114, respectively.

3.1.2 PDP measurements

3.1.2.1 Effect of [NaCl]. Fig. 3 illustrates the PDP curves (in the form of Tafel plots) for the corrosion of the examined brass alloy at diverse [NaCl] (1.5%, 2.5%, 3.5% and 4.5%) at 298 K. The values of corrosion parameters such as the corrosion potential, E_{corr}, cathodic and anodic Tafel slopes, β_a and β_c, respectively, and corrosion current density, i_{corr}, were evaluated by the extrapolation of both branches of the Tafel curves and are inserted in Table 1. Due to the inverse proportionality between R_p and i_{corr}, the calculation of the values of R_p (listed in Table 1) is a valuable method to evaluate the corrosion resistance of a metal/solution system. The figure and the data listed in Table 1 illuminate that increasing the concentration of the corrosive solution (NaCl) shifts both anodic and cathodic branches of the Tafel curves to higher i_{corr}, signifying an increase in the corrosion rate of the alloy. Also, in agreement with the OCP measurements, there is a negative shift in the value of E_{corr} with rising NaCl concentration. The obtained values of both β_a and β_c are found to decrease with rising [NaCl]. The i_{corr} value of the

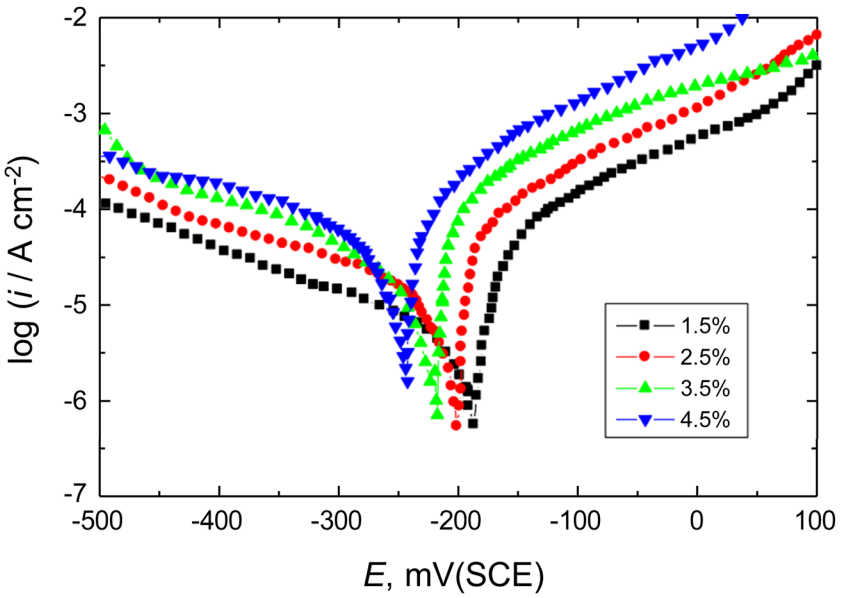

Fig. 3 PDP plots for the corrosion of brass at diverse [NaCl] at 298 K.

Table 1 Corrosion parameters for the corrosion of brass at diverse [NaCl] at 298 K

C_{NaCl} (%)	E_{corr} (mV(SCE))	β_a (mV dec^{-1})	$-\beta_c$ (mV dec^{-1})	i_{corr} (μA cm^{-2})	R_p (ohm cm^2)
1.5	−184	173	228	13.77	3105
2.5	−202	169	323	22.08	2185
3.5	−221	166	153	33.45	1035
4.5	−241	142	183	48.16	722

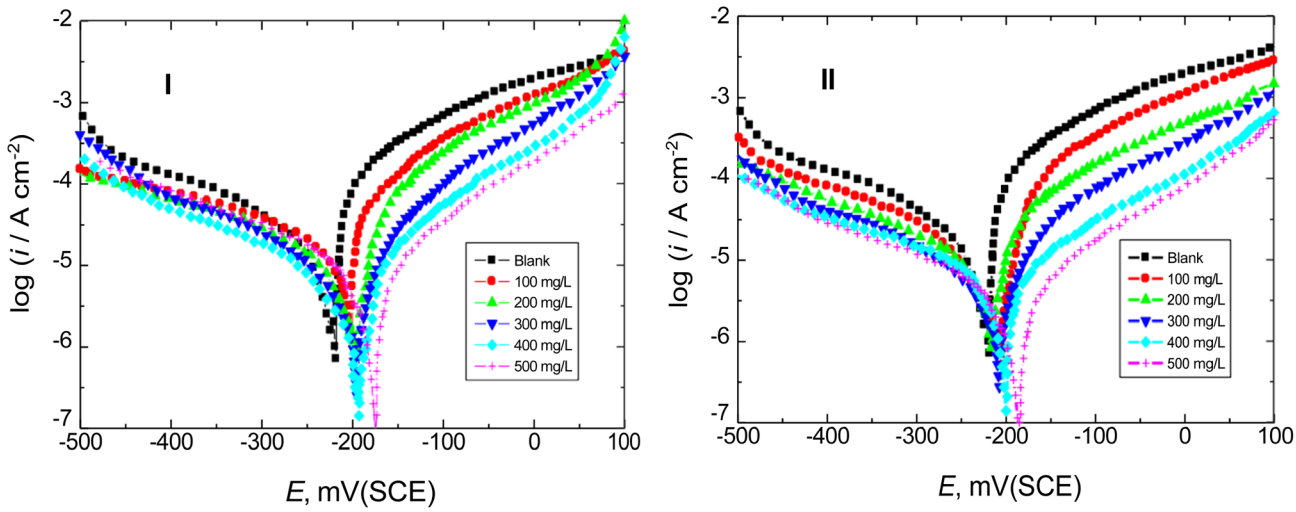

Fig. 4 PDP plots for the corrosion of brass in 3.5% NaCl (blank) and in the presence of streptomycin (I) and neomycin (II) at 298 K.

alloy is found to increase while that of R_p reduces with rising [NaCl], indicating an increase in the corrosion rate with increasing [NaCl], and this trend can be ascribed to the contribution of the adsorbed Cl^- ions on the alloy surface, resulting in the prevention or destruction of the passive film on the alloy surface.

3.1.2.2 Effect of the inhibitor concentrations. PDP measurements were performed for the corrosion of the examined brass alloy in a 3.5% NaCl solution (blank) in the absence and presence of diverse doses (100–500 mg L^{-1}) of streptomycin (I) and neomycin (II) at 298 K, and the Tafel curves are shown in Fig. 4, and the related corrosion parameters are computed and are inserted in Table 2. In addition, the inhibition efficiencies (% IEs) and the degree of surface coverage (θ) of the drugs are calculated *via* eqn (10) (ref. 87) and are listed in Table 2.

$$\%, \mathrm{IE} = \theta \times 100 = \left[1 - \frac{i_{corr(inh)}}{i_{corr}}\right] \times 100 \quad (10)$$

where i_{corr} and $i_{corr(inh)}$ refer to the i_{corr} values in the absence and presence of the drug inhibitors, respectively.

The experimental results denoted that the addition of the expired drugs to the NaCl solution moved the Tafel curves to lower i_{corr} values, indicating a reduction in the rate of corrosion of the examined brass alloy and hence the inhibition of its corrosion. Also, the examined drugs were found to slightly shift the value of E_{corr} of brass in the blank solution towards

Table 2 Corrosion parameters of brass in 3.5% NaCl (blank) and in the presence of streptomycin (I) and neomycin (II) at 298 K

3.5% $NaCl^+$	Inh. conc. (mg L^{-1})	E_{corr} (mV(SCE))	β_a (mV dec^{-1}.)	$-\beta_c$ (mV dec.$^{-1}$)	i_{corr} (μA cm^{-2})	R_p (ohm cm^2)	% IE	θ
Blank	0	−221	166	153	33.45	1035	—	—
Streptomycin (I)	100	−202	112	227	15.21	2144	54.5	0.545
	200	−197	102	161	10.51	2583	68.6	0.686
	300	−193	107	172	7.17	4001	78.6	0.786
	400	−189	136	158	5.52	5756	83.5	0.835
	500	−177	127	175	4.08	7842	87.8	0.878
Neomycin (II)	100	−210	152	170	14.25	2448	57.4	0.574
	200	−214	163	166	9.94	3597	70.3	0.703
	300	−208	149	161	7.14	4712	78.7	0.787
	400	−199	151	174	4.49	7828	86.6	0.866
	500	−184	139	179	2.88	11 812	91.4	0.914

the positive (anodic) direction, indicating that the tested drugs displayed mixed-type inhibition characteristics with an anodic priority.[88] The calculated values of β_a were found to decrease while those of β_c increased in the presence of the examined drugs, demonstrating that the kinetics of the anodic reaction were retarded by the added drugs, while those of the oxygen reduction reaction (cathodic reaction) were accelerated. The value of i_{corr} of the alloy in the blank solution reduced while the R_p value increased with increasing drug dosage, signifying the inhibition of the alloy corrosion. At 500 mg L^{-1} of the tested drugs, the % IEs of drugs I and II were found to be 87.4% and 91.6%, respectively. Thus, the expired drugs acted as efficient inhibitors for the corrosion of the examined brass alloy in a 3.5% NaCl solution.

3.2 Weight loss (WL) measurements

3.2.1 Effect of the inhibitor concentrations. WL tests were done for brass sheets in a 3.5% NaCl medium (blank) and with diverse doses (100–500 mg L^{-1}) of streptomycin (I) and neomycin (II). The plots of WL *vs.* immersion time at 298 K are illustrated in Fig. 5. The values of the corrosion rates (CR) of the alloy were calculated (in mpy) using eqn (11):[89]

$$CR = \frac{KW}{Atd} \quad (11)$$

where K is a constant (3445.15), W is the WL of the alloy (g), A is the brass sheet's area (cm^2), t is the rinsing time (h), and d is the brass alloy's density[90] (8.52 g cm^{-3}).

The values of both % IEs and θ of the expired drugs were calculated by eqn (12):[91]

$$\%IE = \theta \times 100 = \left[\frac{1 - CR_{inh}}{CR}\right] \times 100 \quad (12)$$

where CR and CR_{inh} are the CRs in the absence and presence of the expired drugs, respectively. The corrosion parameters (CR, % IEs and θ) are presented in Table 3. The parameters included in Table 3 indicated that as the drug doses increased, the CR of

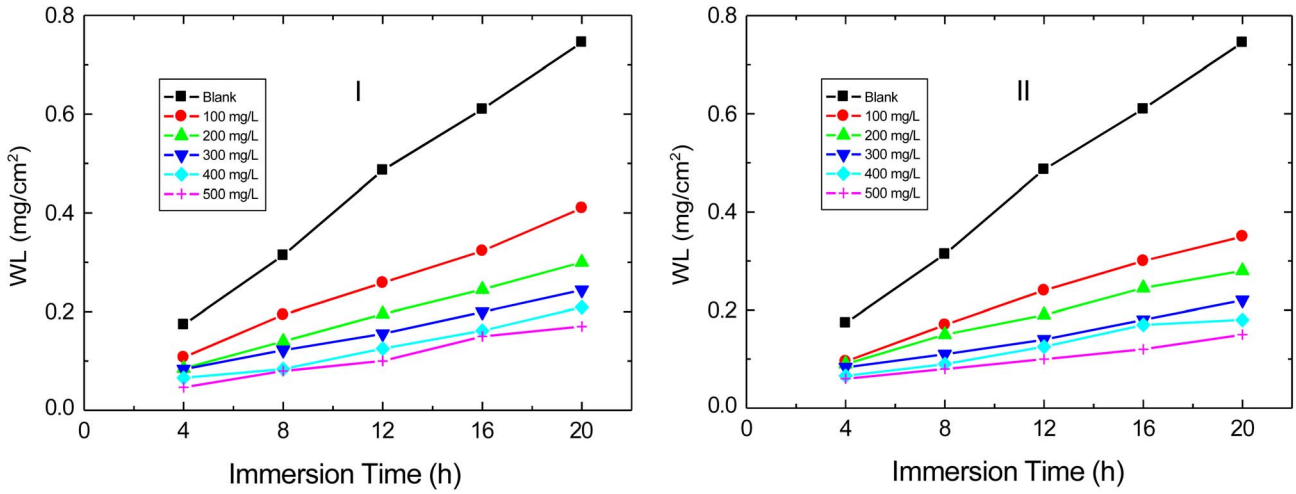

Fig. 5 WL *vs.* time plots for the corrosion of brass in 3.5% NaCl with diverse doses of streptomycin (I) and neomycin (II) at 298 K.

Table 3 Values of the CR of brass in 3.5% NaCl (blank) and % IE and θ values of streptomycin (I) and neomycin (II) at diverse temperatures

		Temperature (K)											
		288			298			308			318		
3.5% NaCl+	Inh. conc. (mg L^{-1})	CR	% IE	θ	CR	% IE	θ	CR	% IE	θ	CR	% IE	θ
Blank	0	16.13	—	—	18.20	—	—	21.89	—	—	26.01	—	—
Streptomycin (I)	100	5.94	63.2	0.632	7.79	57.2	0.572	11.08	49.4	0.494	14.96	42.5	0.425
	200	4.03	75.0	0.750	5.22	71.3	0.713	8.82	59.7	0.597	11.68	55.1	0.551
	300	2.82	82.5	0.825	4.04	77.8	0.778	6.26	71.4	0.714	9.62	63.0	0.630
	400	2.03	87.4	0.874	2.71	85.1	0.851	5.43	75.2	0.752	7.91	69.6	0.696
	500	1.58	90.2	0.902	2.38	86.9	0.869	4.62	78.9	0.789	7.49	73.2	0.712
Neomycin (II)	100	4.87	69.8	0.698	6.79	62.7	0.627	10.09	53.9	0.539	14.64	43.7	0.437
	200	3.32	79.4	0.794	4.15	77.2	0.772	6.83	68.8	0.688	11.91	54.2	0.542
	300	1.92	88.1	0.881	3.09	83.0	0.830	5.45	75.1	0.751	8.74	66.4	0.664
	400	1.55	90.4	0.904	2.29	87.4	0.874	4.84	77.9	0.779	7.26	72.1	0.721
	500	1.13	93.0	0.93	1.87	89.7	0.897	4.07	81.4	0.814	6.55	74.8	0.748

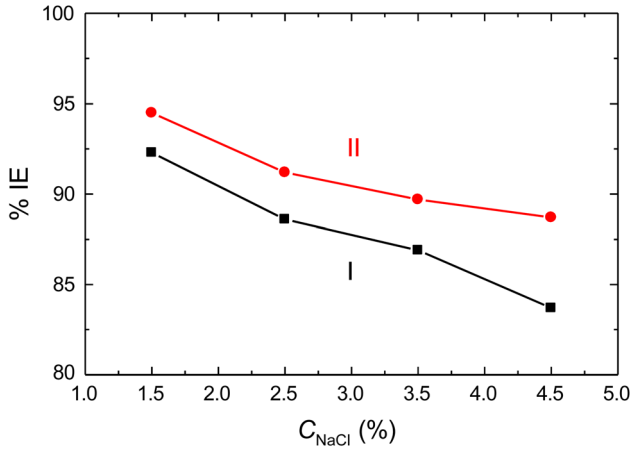

Fig. 6 Variation in the % IEs of streptomycin (I) and neomycin (II) at 500 mg L^{-1} with [NaCl] in the corrosion of brass in NaCl solutions at 298 K.

the alloy reduced, and the % IEs of the tested drugs enhanced. In accordance with PDP measurements, the % IE values of streptomycin (I) were set to be lower than those of neomycin (II), indicating the reality of the investigational outcomes collected from the two employed techniques.

3.2.2 Effect of NaCl concentration on the % IE values. The effect of the concentration of NaCl on the % IEs of streptomycin (I) and neomycin (II) at 500 mg L^{-1} is illustrated in Fig. 6. The figure illustrates that the % IE values decreased with increasing [NaCl], indicating that the expired drugs were more efficient at lower NaCl concentrations.

3.2.3 Effect of the immersion time. To investigate the effect of the immersion time on the values of % IEs of streptomycin (I) and neomycin (II) in the corrosion of brass alloy in 3.5% NaCl, brass sheets were immersed in such a solution with 500 mg L^{-1} of the tested drugs for 4–20 hours at 298 K. The obtained results (illustrated in Fig. 7) showed that the values of

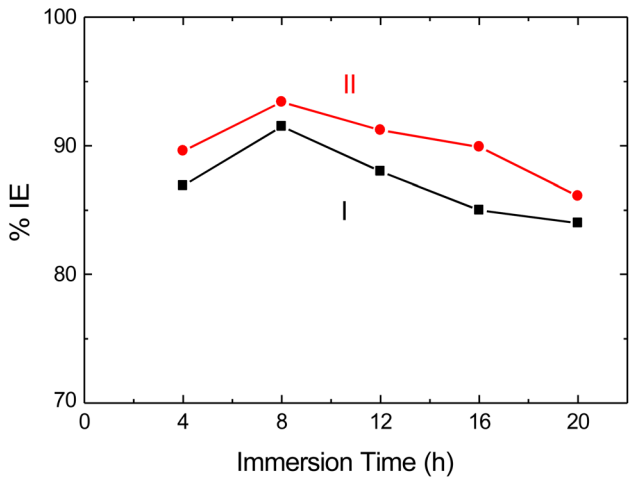

Fig. 7 Variation in the % IEs of streptomycin (I) and neomycin (II) at 500 mg L^{-1} with immersion time in the corrosion of brass in 3.5% NaCl at 298 K.

% IEs improved significantly in the initial stage up to 8 h and subsequently diminished with further lapse of time (8–20 h). The increase in the % IE values in the early stage of immersion may be attributed to the adsorption of drug molecules on the alloy surface and the subsequent improvement in % IEs. After ~8 h, some adsorbed drug molecules are expected to desorb from the alloy surface, resulting in a decrease in the effective area covered by such molecules, causing a reduction in the % IE values.[92]

3.2.4 Effect of temperature. The results of the effect of temperature (listed in Table 3) indicated that the CR of brass in 3.5% NaCl was found to increase, while the % IEs of the expired drugs decreased with increasing temperature, as shown in Fig. 8 and 9, respectively. This performance proposed that the adsorption type of the tested drugs on the brass surface was physical.[93,94]

3.2.5 Adsorption isotherm evaluations. The obtained outcomes from both PDP and WL techniques indicated that the examined expired drugs exerted their inhibition effect *via* their adsorption on the brass alloy's surfaces. Consequently, a study of the various adsorption isotherms is necessary to recognize the nature of the drug molecules' adsorption on the alloy surface. In this context, tests were performed to fit the obtained data with diverse adsorption isotherms, such as Temkin, Langmuir, Freundlich, Frumkin, and Flory–Huggins. The outcomes collected at diverse temperatures signified that the finest fit obeyed the Langmuir isotherm (Eq. (13)),[95] with almost unit slopes gained, as presented in Fig. 10.

$$\frac{C_{inh}}{\theta} = \frac{1}{K_{ads}} + C_{inh} \quad (13)$$

The values of the adsorption constant, K_{ads}, were evaluated from Fig. 10 and are listed in Table 4. The greater K_{ads} values obtained implied the strong and spontaneous adsorption of the drug molecules. Such adsorption is suggested to be physical, where rising solution temperature results in a reduction in the value of K_{ads}.

3.2.6 Thermodynamic parameters. The standard free energy of adsorption (ΔG°_{ads}) was calculated using the equation:[96]

$$\Delta G^{\circ}_{ads} = -RT \ln(55.5\ K_{ads}) \quad (14)$$

The computed ΔG°_{ads} values are listed in Table 4 and were found to be in the range from −30.47 kJ mol^{-1} to −31.92 kJ mol^{-1}, signifying that the adsorption nature was a mixed-type (physicochemical adsorption).[97,98] This adsorption was spontaneous because of the obtained negative values of ΔG°_{ads}.[99] Also, the ΔG°_{ads} values for streptomycin were somewhat lower than those for neomycin, indicating that streptomycin was less adsorbed on the brass alloy surface than neomycin, confirming the obtained % IE values for both drugs.

The values of the standard heat of adsorption (ΔH°_{ads}) were computed using eqn (15):[100]

$$\ln K_{ads} = \frac{-\Delta H^{\circ}_{ads}}{RT} + \text{constant} \quad (15)$$

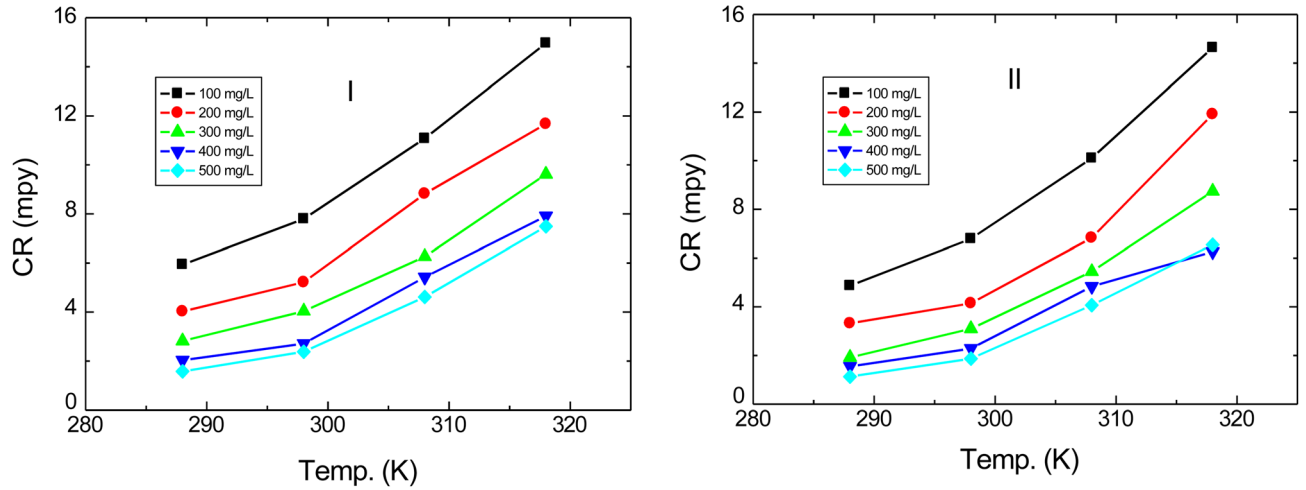

Fig. 8 Variation in the CR of brass in 3.5% NaCl with diverse doses of streptomycin (I) and neomycin (II) with temperature.

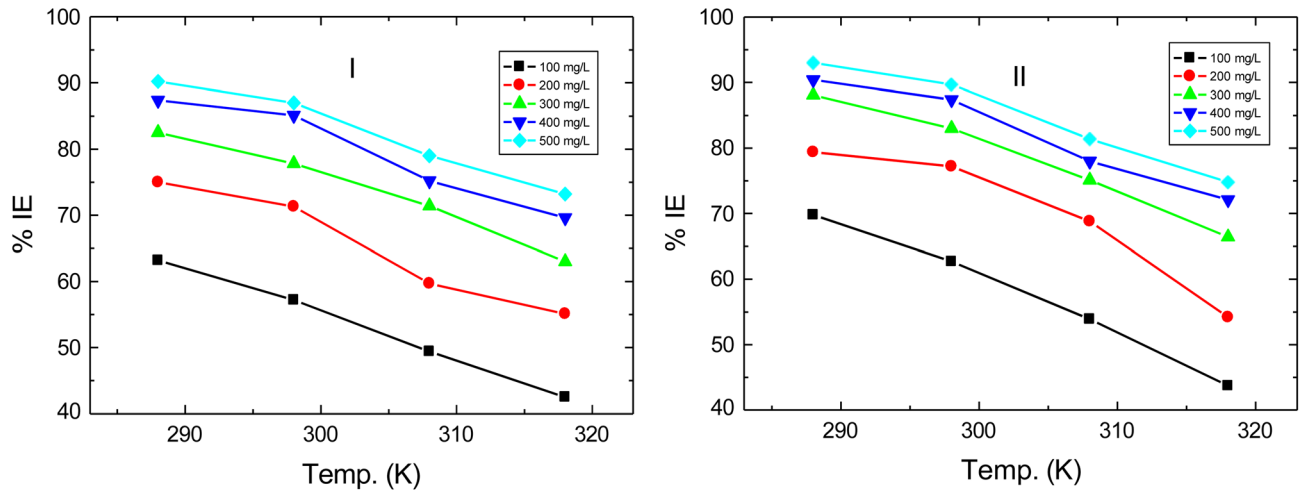

Fig. 9 Variation in the % IEs of diverse doses of streptomycin (I) and neomycin (II) with temperature in the corrosion of brass in 3.5% NaCl.

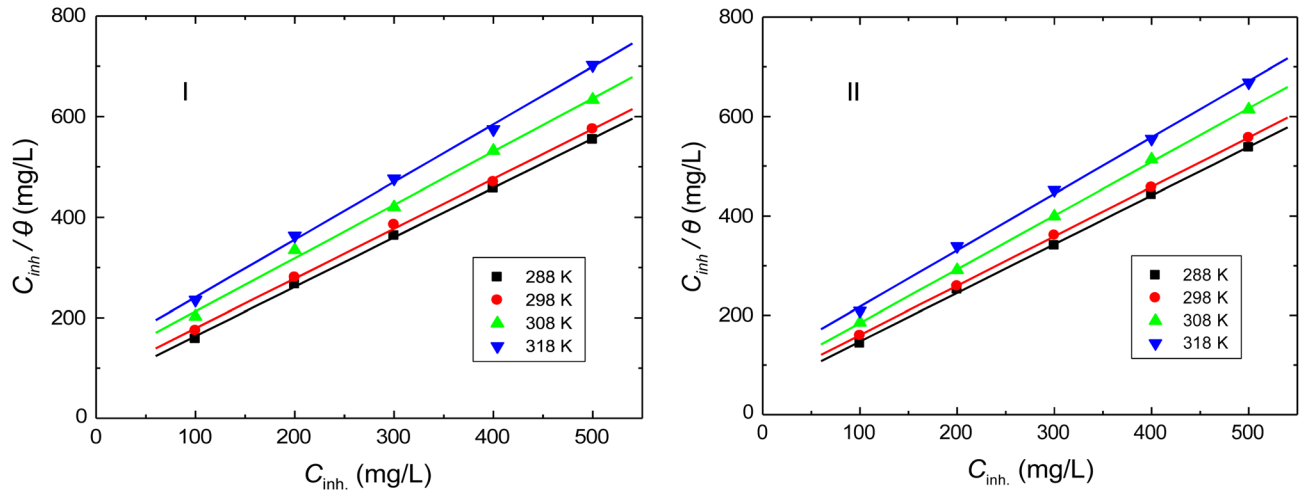

Fig. 10 Langmuir adsorption isotherms for streptomycin (I) and neomycin (II) adsorbed on the surface of brass in 3.5% NaCl at diverse temperatures.

Table 4 Thermodynamic parameters and K_{ads} values for the corrosion of brass in 3.5% NaCl with streptomycin (I) and neomycin (II) at diverse temperatures

3.5% NaCl+	Temp. (K)	10^{-3} K_{ads} L mol^{-1}	ΔG°_{ads} kJ mol^{-1}	ΔH°_{ads} kJ mol^{-1}	ΔS°_{ads} J mol^{-1} K^{-1}
Streptomycin (I)	288	6.06	−30.47	−17.09	71.75
	298	4.99	−31.05		71.26
	308	3.77	−31.37		70.01
	318	3.15	−31.92		69.52
Neomycin (II)	288	8.16	−31.19	−19.11	81.44
	298	6.67	−31.77		80.67
	308	5.19	−32.19		79.42
	318	3.85	−32.45		77.73

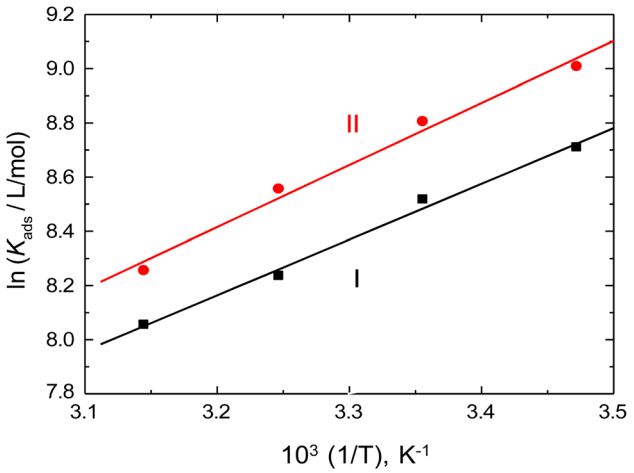

Fig. 11 van't Hoff plots for streptomycin (I) and neomycin (II) adsorbed on the surface of brass in 3.5% NaCl.

Fig. 11 shows the linear plots of ln K_{ads} *vs.* 1/T. The computed values of ΔH°_{ads} (Table 4) were negative, proposing that the adsorption of drug molecules was exothermic with a physical type.[101–104]

The standard entropy of adsorption (ΔS°_{ads}) was calculated using eqn (16):

$$\Delta G^{\circ}_{ads} = \Delta H^{\circ}_{ads} - T\Delta S^{\circ}_{ads} \quad (16)$$

The computed values of ΔS°_{ads} are listed in Table 4, and they signified an increase in the disorder of the adsorption of drug molecules due to the desorption of some H_2O particles from the brass surface, which are substituted by the drug molecules.[103,104]

3.2.7 Kinetic parameters. The activation energy (E_a*) was determined using eqn (17):[102]

$$\ln \mathrm{CR} = \ln A - \frac{E^*_a}{RT} \quad (17)$$

The results indicated that the graphs of ln CR *versus* $1/T$ were linear, as illustrated in Fig. 12, from which E_a* values were evaluated and are inserted in Table 5. The values in the presence of the tested drugs were greater than those obtained in the inhibitor-free medium (blank), signifying the strong physical adsorption of the drugs on the brass surface. Also, the obtained E_a* values were smaller than the 80 kJ mol^{-1} required for

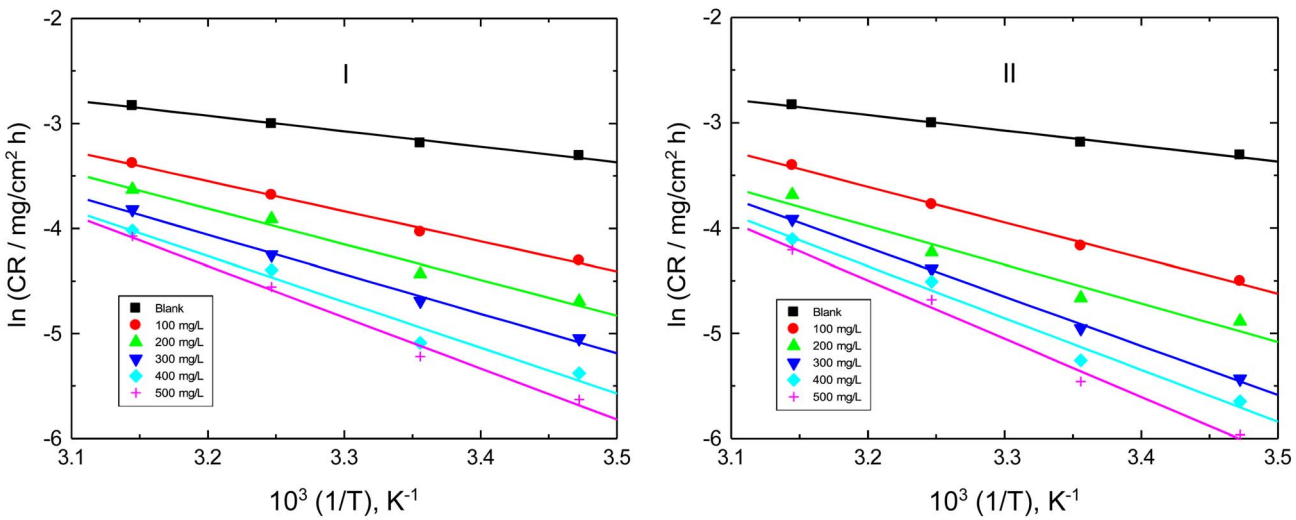

Fig. 12 Arrhenius plots for the corrosion of brass in 3.5% NaCl with streptomycin (I) and neomycin (II).

Table 5 Activation parameters in the corrosion of brass in 3.5% NaCl with streptomycin (I) and neomycin (II)

3.5% NaCl+	Inh. conc. (mg L^{-1})	E_a* kJ mol^{-1}	ΔH* kJ mol^{-1}	ΔS* J mol^{-1} K^{-1}
Blank	0	12.28	9.78	64.44
Streptomycin (I)	100	23.82	21.31	32.85
	200	28.27	25.81	20.37
	300	31.26	28.80	12.89
	400	36.25	33.84	−1.24
	500	40.57	38.13	−13.72
Neomycin (II)	100	28.10	25.59	19.54
	200	30.68	28.06	32.43
	300	37.25	36.44	−10.39
	400	40.93	38.50	−15.38
	500	46.06	43.54	−30.35

chemisorption, revealing that the nature of adsorption was physical.[104]

The values of both activation enthalpy (ΔH*) and activation entropy (ΔS*) were computed using eqn (18):[105]

$$\ln\left(\frac{CR}{T}\right) = \left(\ln\frac{R}{Nh} + \frac{\Delta S^*}{R}\right) - \frac{\Delta H^*}{R} - \frac{1}{T} \quad (18)$$

The ln(CR/T) *vs.* 1/T graphs were linear, as shown in Fig. 13. Table 5 lists the ΔH* and ΔS* values, which were computed from the graphs. The ΔH* values were discovered to be positive, proving that the corrosion process was endothermic, whereas there was a decrease in the ΔS* values, signifying a reduction in the randomness as a result of activated complex establishment.[106] Fig. 14 shows the harmonizing of the trend of E_a* and ΔH* values for both tested drugs.

3.2.8 Corrosion kinetics of the brass alloy. The kinetics of brass corrosion in the tested medium and its inhibition by streptomycin (I) and neomycin (II) at different concentrations were investigated at 298 K. The outcomes displayed that the kinetics of brass corrosion and its inhibition were first-order, as represented by the equation:

$$-\ln \mathrm{WL} = k_1 t - \ln A \quad (19)$$

where k_1 is a first-order rate constant. The linear graphs of –ln WL *vs.* immersion time (t) are illustrated in Fig. 15, indicating that the kinetics of brass corrosion followed a negative first-order. The k_1 values (Table 6) were computed from Fig. 16. Also, the values of the half-life time, $t_{1/2}$, of corrosion were computed using k_1 values using eqn (20):[107]

$$t_{1/2} = \frac{0.693}{k_1} \quad (20)$$

Furthermore, the order of corrosion inhibition, n, was determined (Table 7) using eqn (21):[108]

$$\log \mathrm{CR} = \log k + n \log C_{\mathrm{inh.}} \quad (21)$$

The graphs of log CR *vs.* log C_{inh} for streptomycin (I) and neomycin (II) were linear (Fig. 16), and the obtained values of n indicated that the corrosion inhibition of brass followed

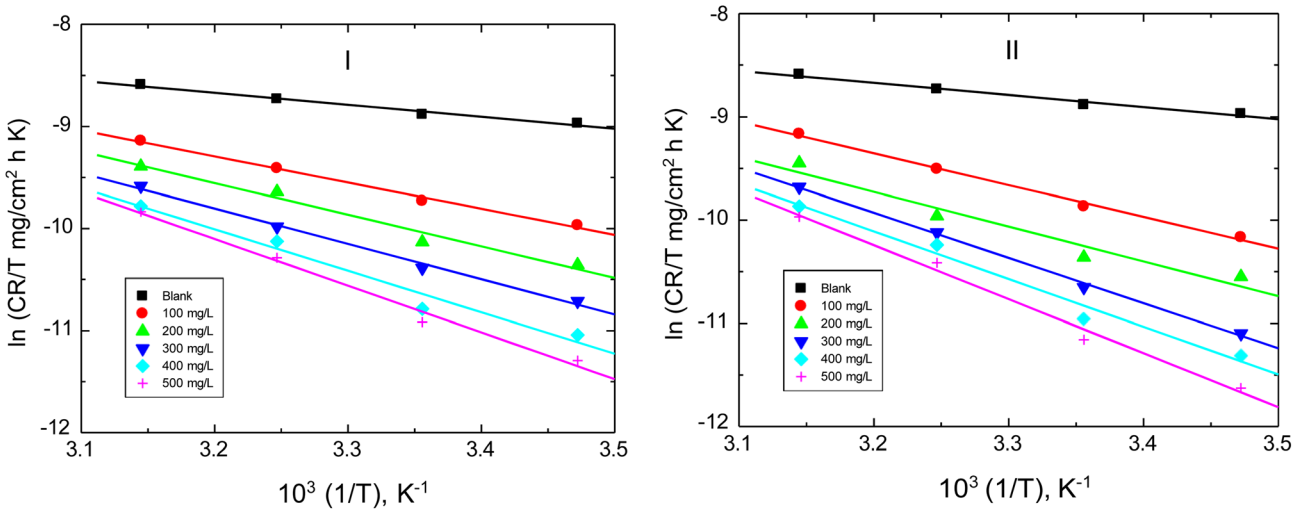

Fig. 13 Transition state plots for the corrosion of brass in 3.5% NaCl with streptomycin (I) and neomycin (II).

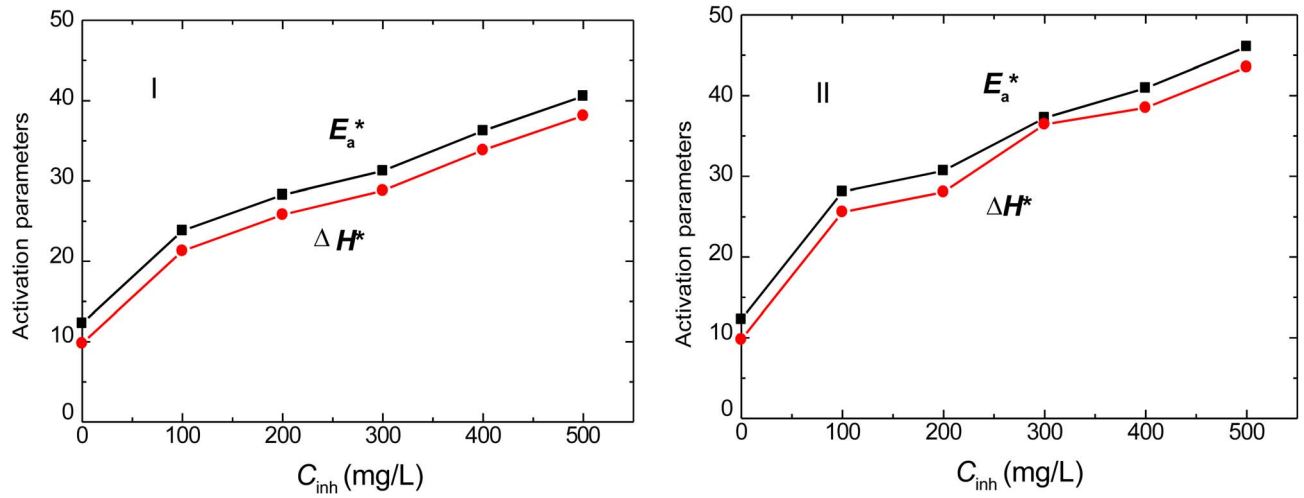

Fig. 14 Variance of E_a* and ΔH* with the concentrations of streptomycin (I) and neomycin (II) in the corrosion of brass in 3.5% NaCl.

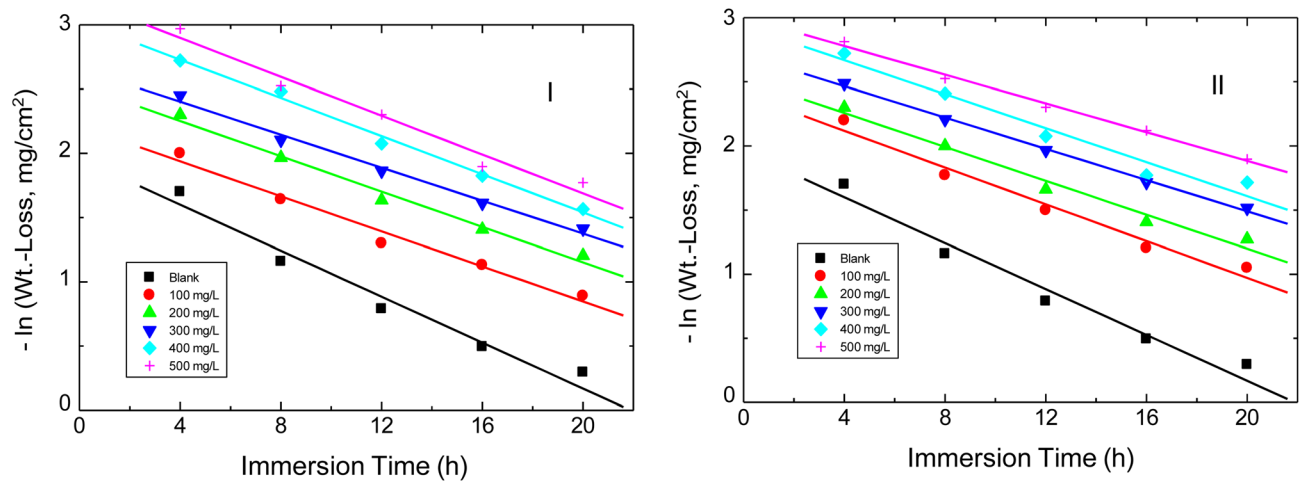

Fig. 15 First-order plots for the corrosion of brass in 3.5% NaCl with streptomycin (I) and neomycin (II) at 298 K.

Table 6 Values of k_1 and $t_{1/2}$ in the corrosion of brass in 3.5% NaCl with streptomycin (I) and neomycin (II) at 298 K

Inh. conc. (mg L^{-1})	Streptomycin (I)		Neomycin (II)	
	k_1, h^{-1}	$t_{1/2}$, h	k_1, h^{-1}	$t_{1/2}$, h
Blank	0.089	7.791	0.089	7.791
100	0.068	10.19	0.071	9.76
200	0.069	10.04	0.066	10.50
300	0.065	10.66	0.061	11.36
400	0.074	9.36	0.066	10.50
500	0.076	9.12	0.056	12.36

a negative fractional first-order with C_{inh}, indicating the good % IEs of the tested drugs.[109]

Finally, according to the comparison of the values of % IEs of the examined drugs, streptomycin (I) and neomycin (II), at 298 K collected *via* the employed techniques (PDP and WL), a decent conformity was accomplished, signifying the validity of the used tools, as presented in Fig. 17.

3.2.9 Surface examination. The SEM photographs of the surfaces of the brass alloy before and after 24 h rinsing with 3.5% NaCl with 500 mg L^{-1} of the tested drugs, streptomycin and neomycin, are presented in Fig. 18A–D, respectively. Fig. 18A presents the surface of refined brass, whereas Fig. 18B presents the brass surface after rinsing with 3.5% NaCl, which shows the damage in the surface and the presence of various pits. Fig. 18C and D show the disappearance of the previously visible damage characteristics from the brass surfaces and the formation of protective layers on them, proving the potent adsorption of the drugs on brass surfaces and establishing excellent inhibitive properties. Hence, the SEM study was in decent conformity with the outcomes obtained from the different employed tools.

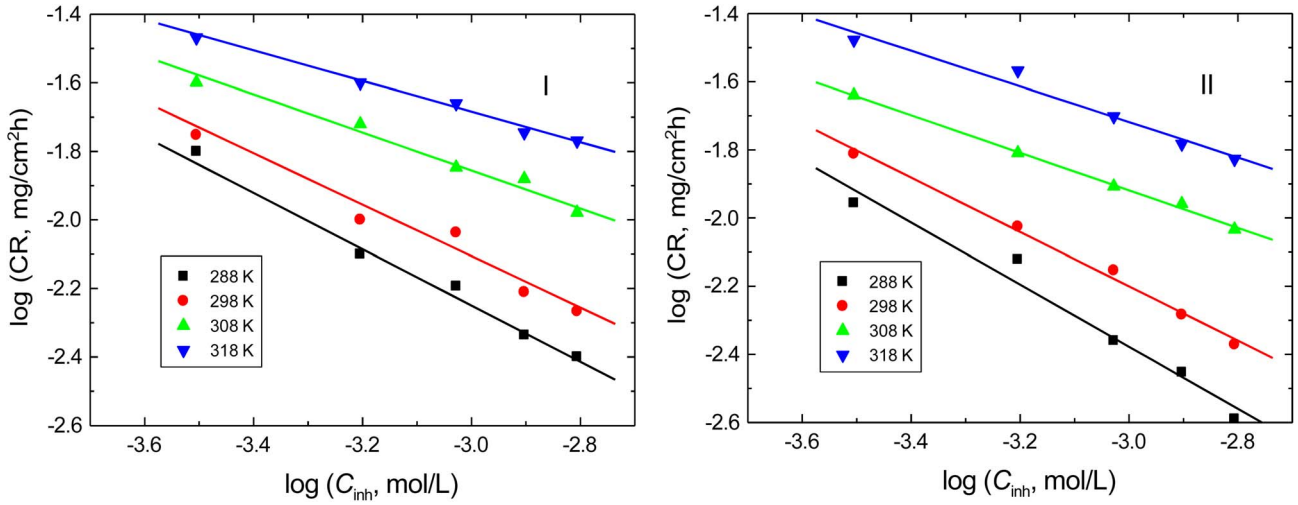

Fig. 16 Plots of log CR *vs.* log C_{inh} for the corrosion inhibition of brass in 3.5% NaCl by streptomycin (I) and neomycin (II) at diverse temperatures.

Table 7 Values of the order, *n*, of corrosion inhibition of brass by streptomycin (I) and neomycin (II) at diverse temperatures

Temp. (K)	Streptomycin (I)	Neomycin (II)
288	−0.821	−0.912
298	−0.751	−0.797
308	−0.556	−0.551
318	−0.445	−0.522

3.3 Theoretical studies

3.3.1 DFT calculations. The compounds' inhibitory function can be linked to heteroatoms that adhere to the brass surface. The contributions of the two examined drugs to the suppression of brass corrosion were demonstrated in the current investigation using quantum chemical parameters. Fig. 19 depicts the two scenarios in which the inhibitors' orbitals (LUMO and HOMO) have the optimal geometric structures (neutral and protonated). A compound's larger E_{HOMO} value indicates its ability to transfer electrons to the unfilled d-orbital of the metal surface, whereas a compound's lower E_{LUMO} value indicates its ability to take electrons.[110] The E_{HOMO} and E_{LUMO} data listed in Table 8 demonstrate that the drugs under examination are capable of giving or receiving electrons. The energy vacuum (ΔE), whose magnitude determines whether inhibitor atoms are reactive after adsorption on the brass surface, is another important component. There is an inverse relationship between the value of ΔE and the reaction that takes place during adsorption. Compounds with low energy gap values make good corrosion inhibitors because an electron may be expelled from their outer shell orbital with a very low ionization energy.[111] Because the inhibitors have a smaller energy gap (ΔE) in their neutral form than in their protonated state,

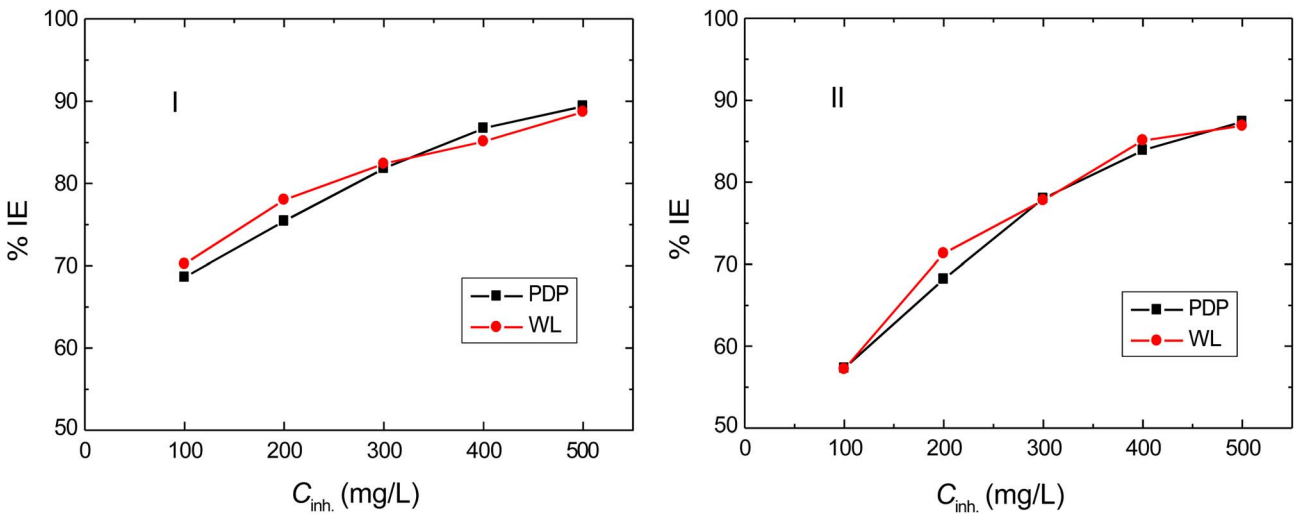

Fig. 17 Comparison of the used techniques (PDP and WL) for the % IE values of streptomycin (I) and neomycin (II) for the corrosion of brass in 3.5% NaCl at 298 K.

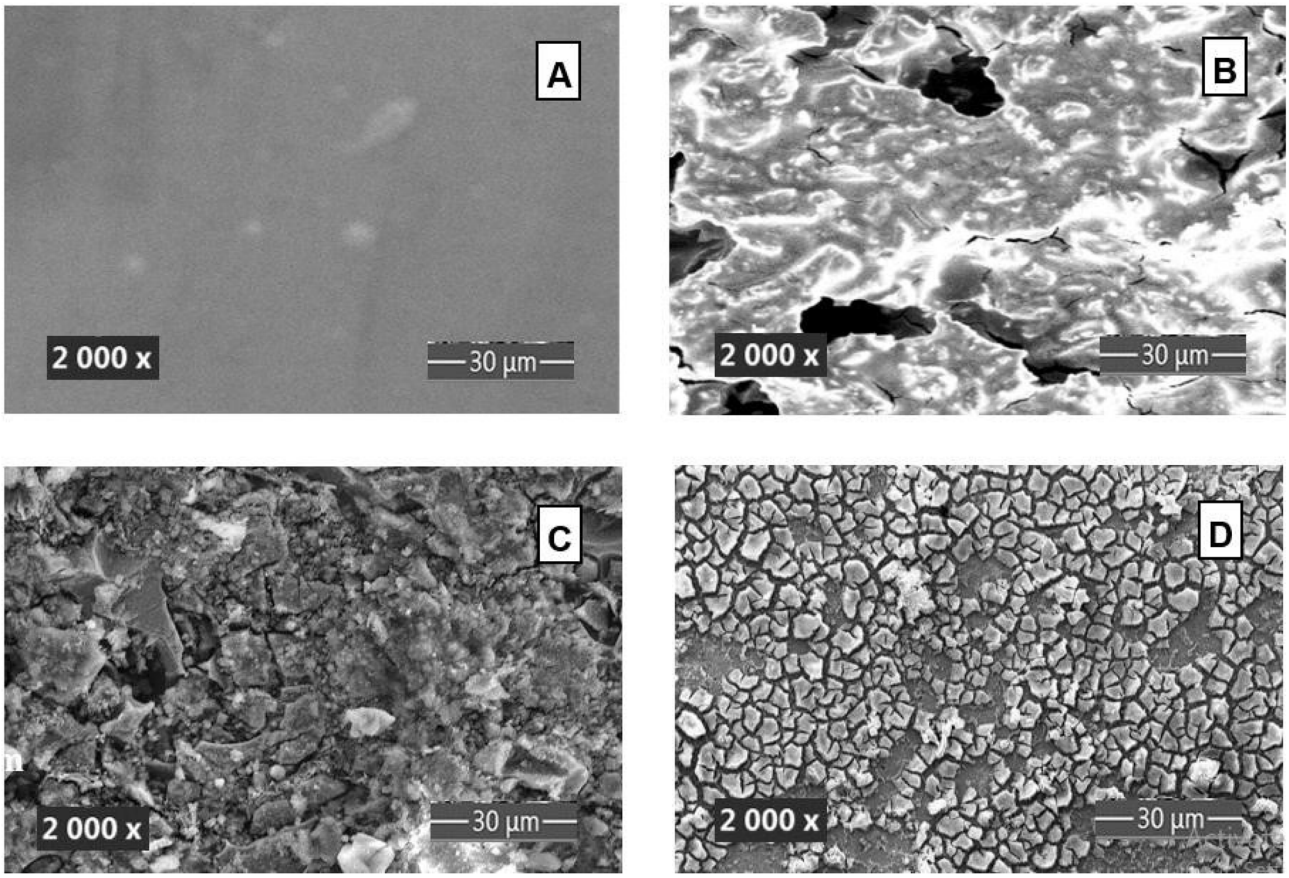

Fig. 18 SEM images (mag. 2000×) of the surfaces of brass (A) before and after 24 hours of immersion in (B) 3.5% NaCl and (C) and (D) 3.5% NaCl with 500 mg L^{-1} streptomycin and neomycin, respectively.

there could be a greater response between the two drugs and the neutral form of the brass surface.[112] The absolute hardness (η) and softness (σ) values may be used to determine the composition, stability, and reactivity of molecules. The easiest electron transfer occurs exclusively in the area of inhibitor molecules, with the highest data becoming an adsorbate.[113] In the process of corrosion, the inhibitor molecules become Lewis bases, while brass becomes a Lewis acid. In fact, organic inhibitor molecules are considered Lewis bases because they play the role of donating lone pairs of electrons to the unoccupied d-orbitals of the metal, *i.e.* they chemically bond to the alloy surface, forming a protective layer and thus preventing corrosion attack. When it comes to moderately acidic bulk metals, soft-base inhibitors are the most efficient way to prevent NaCl corrosion. The structure is shifted and made more logical using the dipole moment.[114,115] When comparing results, the possibility that stronger interactions between the inhibitor molecules and the brass surface resulted in a higher % IE and better adsorption is taken into account. The electrostatic interaction between an excited brass surface and an organic dipole causes the organic dipole to be physically adsorbed onto the alloy surface. Thus, the drug molecules with greater dipole moment values are preferred. When dipole moments were measured, it was found that protons significantly changed the shape of the dipole torque,[116] indicating that the examined drugs are as securely bonded to the brass surface as a proton can be. Nevertheless, there is no proof in the literature that the inhibitory efficacy is related.[117] The ability of the electronic inhibitor on the brass surface is said to increase the inhibition efficiency if ΔN is less than 3.6.[118] It's worth noting that the higher the electronegativity (χ) of an inhibitor, the greater its tendency to attract electrons to the metal surface. This is a quantitative chemical criterion for predicting the inhibitor's effectiveness in adsorption and corrosion prevention. As electronegativity χ_{inh} rises, so does the propensity to be adsorbed on a copper surface and prevent corrosion. Table 9 shows the drugs' inhibitory effects in relation to the previous study.[119] Neomycin molecules have a stronger inhibitory effect by increasing the region in which those molecules may interact with the brass surface. We discovered that the proton form of the two examined drugs had higher numerical values than the neutral form, in terms of the nucleophilicity index (ε). As a result, both drugs are highly nucleophilic in their protonated states. This illustrates how the proton shape might help electrons adhere to the brass surface. The electro-accepting power ($\omega^{+} = (I + 3A)^2/16(I - A)$) and electro-donating power ($\omega^{-} = (3I + A)^2/16(I - A)$) have recently been used to assess the capacity of inhibitors to deliver or receive electrical charge, respectively.[120] Important indicators of

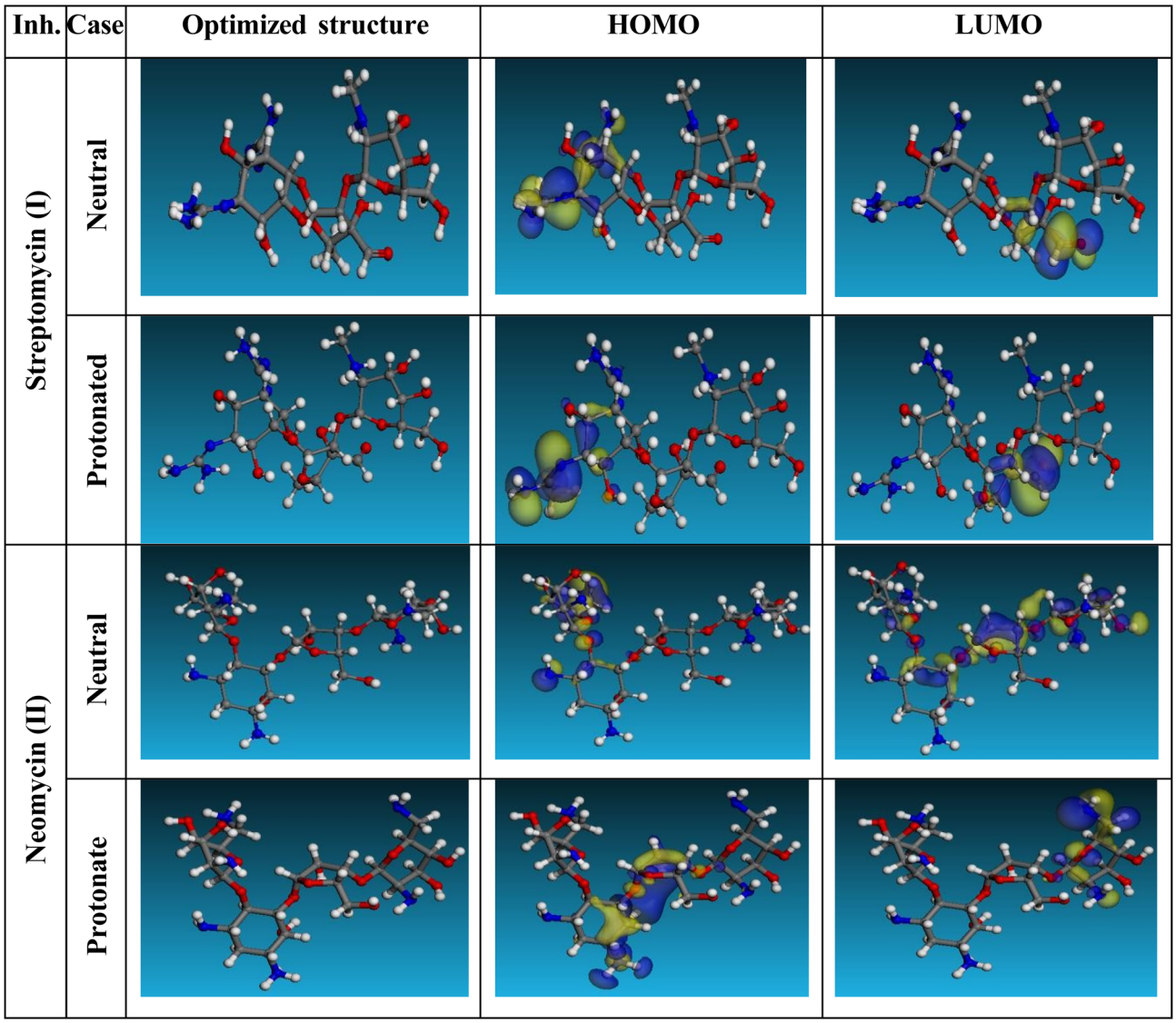

Fig. 19 HOMO and LUMO orbital shapes and molecular structure optimization of streptomycin (I) and neomycin (II) in their neutral and protonated forms in the corrosion of brass in 3.5% NaCl.

electron donation and charge transfer from brass to the inhibitor molecules are the positive values of hardness (η) and, consequently, the negative values of the back-donation energy (E back-donation $= -\eta/4$).

3.3.2 MD simulation. The adsorption process and the attraction between the inhibitor species and the brass alloy surface were investigated using Monte Carlo simulations. The ideal adsorption configurations of drug molecules on the brass surface in a 3.5% NaCl solution are depicted in the adsorption location module in Fig. 20. This suggests maximum surface coverage and improved adsorption.[121] The adsorption energies, which are crucial, were calculated and are inserted in Table 9. It was found that neomycin molecules have a more negative adsorption energy value (-5288.68 kcal mol^{-1}) than streptomycin molecules (-4368.299 kcal mol^{-1}). Also, in the protonated case, neomycin has a higher value of adsorption energy than streptomycin. The values for the neutral and protonated cases of the two examined drugs are high. These values indicate that their adsorption on the brass surface is high, and such adsorption is a mixed-type (physical and chemical adsorption).[122] The protonation of the inhibitor molecules enhances their anti-corrosion performance by increasing their ability to adsorb onto the metal surface and prevent corrosion. In a neutral environment, *e.g.* a 3.5% NaCl solution, the protonation of the inhibitor is likely to occur either by:

(i) In an aqueous 3.5% NaCl solution, Zn–Cu dissolves to form metal ions (*e.g.*, $Zn \rightarrow Zn^{2+} + 2e^{-}$) and thus releases electrons (anodic reaction). At the same time, water is reduced ($2H_2O + 2e^{-} \rightarrow H_2(g) + 2OH^{-}$), and the number of OH^{-} ions increases at the cathode, creating a local alkaline environment (cathodic reaction). The metal ions produced at the anode can then react with electrolyte ionic species (OH^{-} and Cl^{-} ions) to form metal hydroxides and chlorides, consuming OH^{-} ions and thus possibly slightly reducing the pH of the bulk solution near

Table 8 Quantum parameters of streptomycin (I) and neomycin (II) in their neutral and protonated forms in the corrosion of brass in 3.5% NaCl

Inhibitor	Parameters	Dissolved, neutral	Protonated
Streptomycin (I)	$-E_{HOMO}$ (eV)	−5.019	−5.096
	$-E_{LUMO}$ (eV)	−2.038	−2.004
	ΔE (eV)	2.71	3.092
	η (eV)	1.355	1.546
	σ (eV)$^{-1}$	0.738	0.646
	P_i (eV)	−3.529	−3.55
	X (eV)	3.529	3.55
	Dipole moment (debye)	14.5	27.9541
	Molecular area (A^2)	508.849	501.469
	ω (electrophilicty index) (eV)	4.596	4.076
	ω^+ (electro-accepting power) (eV)	6.127	6.044
	ω^- (electro-donating) (eV)	2.599	2.494
	ε (nucleophilicity index) (eV)$^{-1}$	0.217	0.245
	ΔE back-donation (eV)	−0.339	−0.386
	ΔN_{max} (e)	1.28	1.12
Neomycin (II)	$-E_{HOMO}$ (eV)	5.195	5.327
	$-E_{LUMO}$ (eV)	0.847	0.409
	ΔE (eV)	4.348	4.918
	η (eV)	2.174	2.459
	σ (eV)$^{-1}$	0.459	0.406
	P_i (eV)	−3.021	−2.868
	χ (eV)	3.021	2.868
	Dipole moment (debye)	16.8956	28.35
	Molecular area (A^2)	541.98	540.866801
	ω (electrophilicty index) (eV)	2.098	1.672
	ω^+ (electro-accepting power) (eV)	3.88	3.41
	ω^- (electro-donating) (eV)	0.860	0.546
	ε (nucleophilicity index) (eV)$^{-1}$	0.477	0.597
	ΔE back-donation (eV)	−0.543	−0.615
	ΔN_{max} (e)	0.915	0.840

Table 9 Theoretical parameters of streptomycin (I) and neomycin (II) molecules calculated using MD simulations in the corrosion of brass in 3.5% NaCl

Inh	Factors	Neutral	Protonated	Vacuum
Streptomycin (I)	Total energy (kcal mol^{-1})	−5351.44	−7595.47	−301.29
	Adsorption energy (kcal mol^{-1})	−4137.40	−41677.98	−161.56
	Rigid adsorption energy (kcal mol^{-1})	−4368.30	−5371.40	−127.69
	Deformation energy (kcal mol^{-1})	230.90	−363.66	−33.87
	dE_{ad}/dN_i (kcal mol^{-1})	−83.69	−710.84	−161.56
	dE_{ad}/dN_i (kcal mol^{-1}) water	−13.21	−29.11	—
Neomycin (II)	Total energy (kcal mol^{-1})	−7611.90	−7610.61	−156.03
	Adsorption energy (kcal mol^{-1})	−5288.70	−5176.79	−195.26
	Rigid adsorption energy (kcal mol^{-1})	−5541.29	−5443.75	−146.10
	Deformation energy (kcal mol^{-1})	252.61	266.96	−49.15
	dE_{ad}/dN_i (kcal mol^{-1})	−234.41	−231.78	−195.26
	dE_{ad}/dN_i (kcal mol^{-1}) water	−13.45	−13.51	—

the anode, creating a pH gradient. Under these conditions, inhibitor molecules may be protonated through heteroatoms (*e.g.* N) in their structure.

(ii) As shown in Fig. 1, streptomycin and neomycin contain multiple functional groups like $-NH_2$ (basic) and OH (acidic) groups. In a neutral solution, these inhibitors can exist as Zwitterions,[13] *i.e.* these basic amino groups can be protonated (becoming positively charged $-NH^{3+}$). In Zwitterions, the positive charges of the amino groups can be balanced by negative charges from deprotonated hydroxyl groups, producing an electrically neutral molecule with both positive and negative charges.

Because the first suggestion requires a lower pH (acidic environment), which is not the case for the corrosion of Zn–Cu in an aqueous NaCl solution, the second possibility is more likely to occur for the protonation of inhibitor molecules in a neutral solution. The protonation of the inhibitor alters the molecule's electron distribution, significantly increasing the dipole moment, enhancing the van der Waals forces, modifying adsorption strength and creating effective positively charged

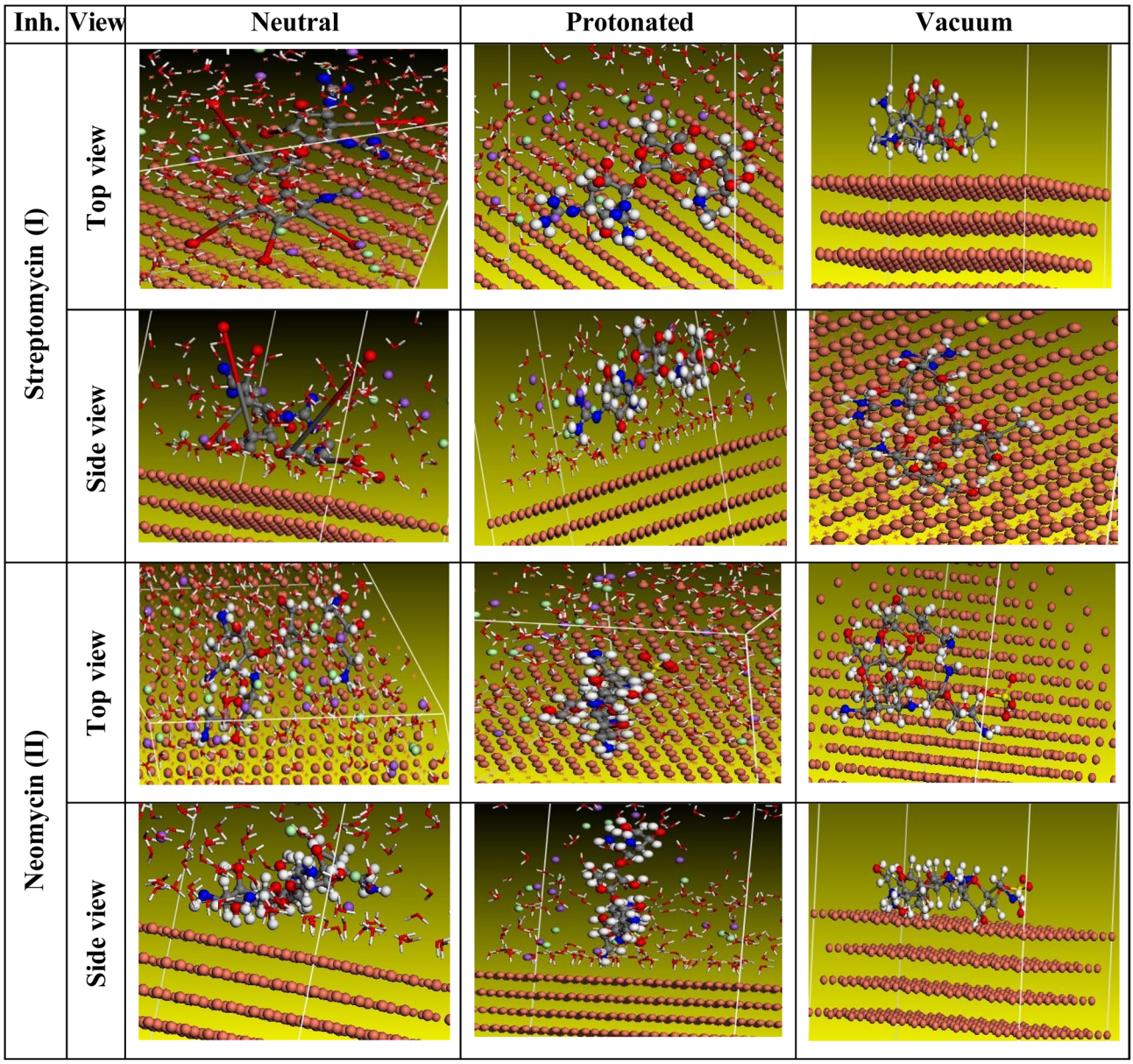

Fig. 20 Adsorption locator module's recommendation for the best formation for the adsorption of streptomycin (I) and neomycin (II) on copper (1 1 1).

molecules. The positively charged inhibitor molecules will then strongly interact electrostatically with the negatively charged brass surface pre-covered with chloride ions.[5,6] This increased attractive force causes the inhibitor molecules to adsorb and cover the metal surface more effectively, thus preventing corrosion more efficiently. As long as the adsorbed inhibitor molecules and additional adsorbate molecules are not included, the dE_{ads}/dN_i values may be used to calculate the energy of the brass/adsorbate configuration.[123] When one of the individual adsorbate particles is separated or removed from its corresponding adsorbent substrate, the energy gained or obtained is measured in kcal mol^{-1} and is mathematically expressed as the differential change in the energy with respect to the change in the number of adsorbate particles or dE_{ads}/dN_i. The data listed in Table 9 indicate that the dE_{ads}/dN_i value of neomycin molecules is larger (-234.41 kcal mol^{-1}) than that of streptomycin molecules (-83.69 kcal mol^{-1}). This suggests that neomycin is more capable of adsorption than streptomycin. Furthermore, water has a dE_{ads}/dN_i value of -13.45. This low value, compared to neomycin molecules, implies that neomycin exhibits better adsorption than ions of water. The notion that neomycin molecules create a robust adsorbed protective layer on the surface of brass, offering corrosion resistance in the studied corrosive environment, is supported by both theoretical and experimental data. When there is an aqueous solution present, the inhibitor molecules adsorb more strongly on the brass surfaces because the related adsorption energies are higher than those seen in a vacuum. To determine how much

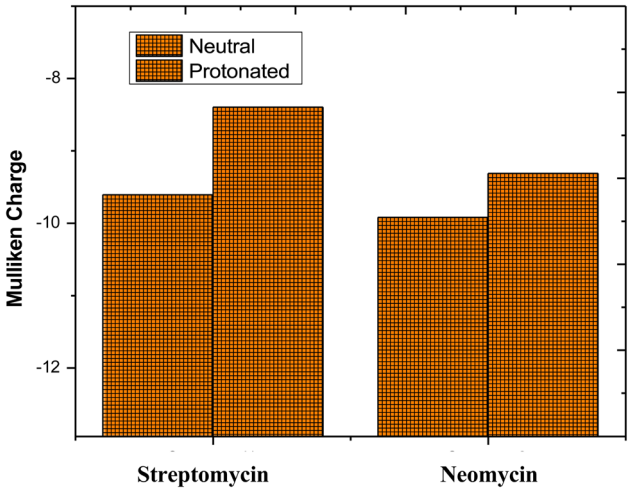

Fig. 21 Mulliken charges of the neutral and protonated streptomycin (I) and neomycin (II) in the corrosion of brass in 3.5% NaCl.

energy CCIBA will adsorb onto the brass surface or copper (111) contact, the following formulas were used:[124,125]

$$E_{\text{binding}} = -E_{\text{interact}} \quad (22)$$

$$E_{\text{interact}} = E_{\text{tot}} - (E_{\text{sub}} + E_{\text{inh}}) \quad (23)$$

Here, E_{sub} represents the energy of water and substrate molecules, while E_{tot} represents the structure's total energy.

3.3.3 Fukui indices and Mulliken charges. The two examined drugs' donor–acceptor active sites are the ones that are most likely to come into contact with the brass alloy surface. A similar pattern of behavior is shown in Fig. 21 and Tables S1–S4 in the SI, where the total negative charge (TNC) increases when the two drugs are protonated.[126] The electrostatic attraction between protonated drugs and chloride ions deposited on the brass surface indicates an increase in the structural interaction of protonated particles. Heteroatoms and other organic materials can protonate in the NaCl solution to create positively charged particles. The Cl^- ions, which are extensively dispersed throughout the alloy surface, interact with these substances. As extra suggestions (Fukui's index (FI)), Fig. 22 and Tables S1–S4 (in the SI file) show the two examined drugs with more data on f^+ and f^- in both neutral and protonated scenarios. According to the findings, every molecule has unique atoms for both nucleophilic and electrophilic systems. The molecule with the greatest f^+, which contains the LUMO, is more reactive to donor reagents and is more likely to be attacked by nucleophiles. Electrophilic attack results from the target reactivities of molecules' atoms towards an acceptor substance due to its greatest values of f^- associated with HOMO. Additionally, the two drugs have a twofold effect because altered atoms in the same drug have different f^+ and f^- values.

3.3.4 MESP. MESP is used to identify the chemical processes that are happening. At various points on the electron density surface, the electrostatic potential is coloured. The region that is indicated in red as electrically active and

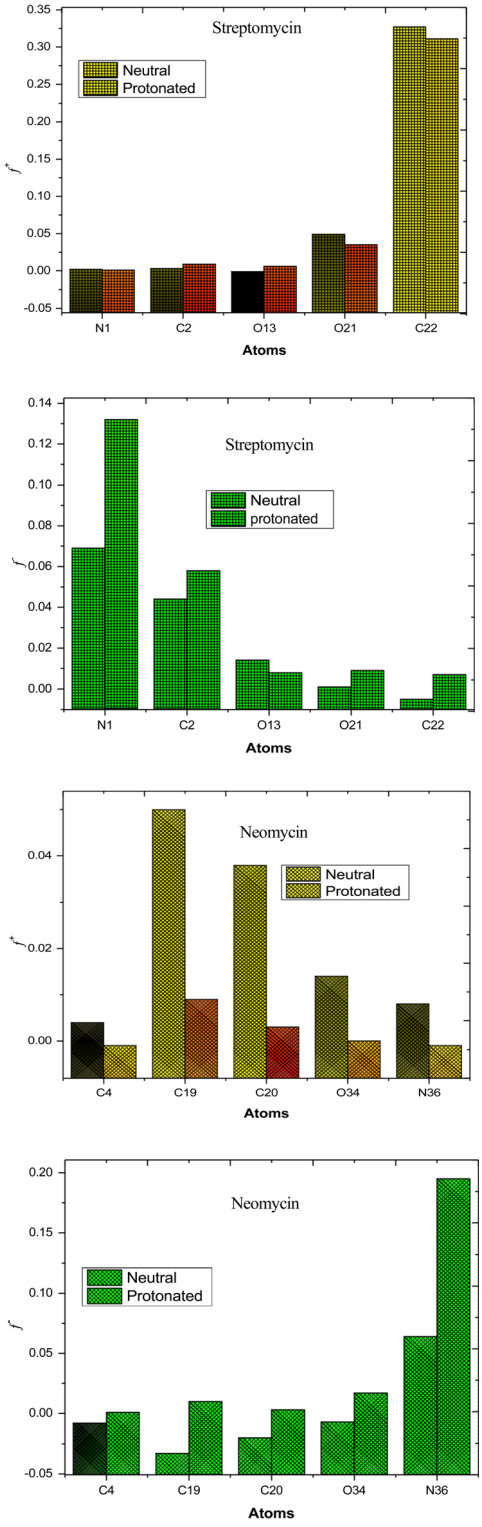

Fig. 22 Graphical depiction of streptomycin (I) and neomycin (II) Fukui indices for their more reactive atoms in their neutral and protonated systems in the corrosion of brass in 3.5% NaCl.

electrophilic mostly has a negative electrostatic potential. Most heteroatoms and double conjugate bonds may be seen in regions with a high electron density. Negative zones that encourage electrophilic attack are shown by oxygen and

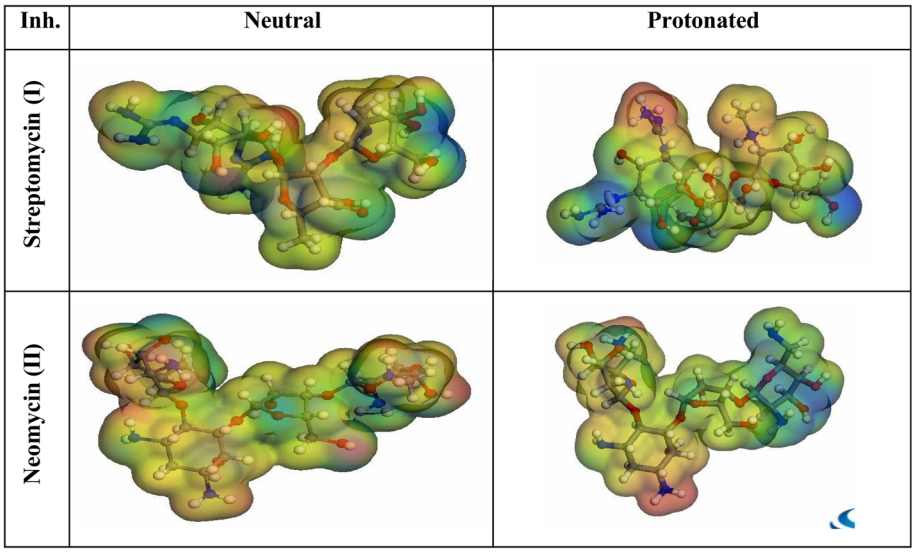

Fig. 23 Electrostatic potentials of streptomycin (I) and neomycin (II) in the corrosion of brass in 3.5% NaCl.

nitrogen. Blue hydrogen atoms are more vulnerable to nucleophile attack, as seen in Fig. 23.

3.3.5 Inhibition mechanism. The cathodic reaction of the brass alloy in NaCl solutions has been reported in the literature[127,128] and is represented by the following equations:

$$2H_2O + 2e^- = H_2 + 2OH^- \quad (24)$$

$$O_2 + 2H_2O + 4e^- = 4OH^- \quad (25)$$

The anodic reactions of brass are the dissolution of its constituents (Cu and Zn).[27]

In the initial stages of the reaction, Zn oxidizes to form ZnO according to the following reactions:[27]

$$Zn = Zn^{2+} + 2e^- \quad (26)$$

$$Zn^{2+} + H_2O = ZnO + 2H^+ \quad (27)$$

Or

$$Zn + H_2O \rightarrow ZnO + 2H^+ + 2e^- \quad (28)$$

Also, Cu oxidizes to form Cu_2O, as follows:[27,129]

$$Cu = Cu^+ + e^- \quad (29)$$

$$2Cu^+ + H_2O \rightarrow Cu_2O + 2H^+ \quad (30)$$

Or

$$2Cu + H_2O \rightarrow Cu_2O + 2H^+ + 2e^- \quad (31)$$

Thus, the brass alloy in NaCl, in the absence of the inhibitors, undergoes oxidation reactions to form the oxides ZnO and Cu_2O as oxidation products, which cover the alloy surface.

In the presence of Cl^- ions, the CuCl is formed on the alloy surface by the reaction:[31]

$$Cu^+ + Cl^- \rightarrow CuCl \quad (32)$$

The formed CuCl layer has poor adhesion, and it slightly protects the alloy surface. Such a layer disproportionates to $CuCl_2$:[130]

$$2CuCl \rightarrow Cu + CuCl_2 \quad (33)$$

Or forms $CuCl_2^-$ complexes[131,132] *via* the reaction:

$$CuCl + Cl^- \rightarrow CuCl_2^- \quad (34)$$

which oxidize, resulting in the dissolution of Cu,

$$CuCl_2^- = Cu^{2+} + 2Cl^- + e^- \quad (35)$$

The better inhibitory effects of the examined drugs, which contain N and O atoms, lead to the creation of a coordination bond amongst the metal and lone pairs of electrons on N and O atoms, leading to the adsorption of the inhibitor molecules on the alloy surface. At lower concentrations of the drugs, they react with CuCl to form the adsorbed layer of the compound $[Cu–Inh.]_{ads}$, according to the following reaction:[132]

$$CuCl_{ads} + Inh. = [Cu–Inh.]_{ads} + Cl^- + H^+ \quad (36)$$

Though, in the presence of higher concentrations, they tend to adsorb directly on the alloy surface *via* the reaction:[133]

$$Cu + Inh. = [Cu–Inh.]_{ads} + e^- \quad (37)$$

Due to such reactions, a shielding layer of $[Cu–Inh.]_{ads}$ is developed on the brass surface, which prevents both further corrosion reactions and adsorption of Cl^- ions on the alloy

surface, resulting in a reduction in the CR and an inhibition of its corrosion. In addition, the adsorption of drugs on the brass surface may be because of the replacement of Cl^- ions or H_2O molecules adsorbed on the brass surface by the drug molecules,[134]

$$Inh._{(sol)} + nH_2O_{(ads)} \leftrightarrow Inh._{(ads)} + nH_2O_{(sol)} \quad (38)$$

resulting in the establishment of a potent shielding layer that protects the alloy surface.[134]

4. Conclusions

1. Herein, the performances of two expired drugs, streptomycin and neomycin, as inhibitors for the corrosion of a high Cu–Zn alloy in a 3.5% NaCl solution were investigated using various electrochemical, gravimetric and microscopic techniques as well as theoretical calculations.

2. The examined expired drugs were discovered to be efficient inhibitors of the corrosion of brass in an NaCl medium.

3. There was an increase in the corrosion rate of brass with rising [NaCl].

4. The % IE values improved with rising drug doses, while they decreased with rising [NaCl] and solution temperature.

5. The % IEs were proposed to be due to the strong adsorption of the drugs on the brass surface, and this adsorption was suggested to be physical and obeyed the Langmuir adsorption isotherm.

6. The drugs were discovered to work as mixed-type inhibitors with an anodic priority.

7. Both thermodynamic and kinetic quantities were evaluated and discussed.

8. The kinetics and mechanisms of brass corrosion in an NaCl medium and its inhibition by the investigated drugs were studied.

9. The applied computational methods provided more insights into the inhibition mechanism of the tested drugs.

10. All outcomes of various applied techniques were in excellent conformity with each other and with the employed computational methods.

Conflicts of interest

There are no conflicts to declare.

Data availability

All the data are included within the manuscript.

Supplementary information is available. See DOI: https://doi.org/10.1039/d5ra06456b.

Acknowledgements

This work was supported and funded by the Deanship of Scientific Research at Imam Mohammad Ibn Saud Islamic University (IMSIU) (grant number IMSIU-DDRSP2502).

References

1 A. Toghan, A. Fawzy, A. I. Alakhras, M. M. S. Sanad, M. Khairy and A. A. Farag, Correlating Experimental with Theoretical Studies for a New Ionic Liquid for Inhibiting Corrosion of Carbon Steel during Oil Well Acidification, *Metals*, 2023, **13**, 862, DOI: 10.3390/met13050862.

2 H. S. Gadow, A. Fawzy, M. Khairy, M. M. S. Sanad and A. Toghan, Experimental and theoretical approaches to the inhibition of carbon steel corrosion by thiophene derivative in 1 M HCl, *Int. J. Electrochem. Sci.*, 2023, **18**, 100174.

3 A. Toghan, O. K. Alduaij, A. Fawzy, A. M. Mostafa, A. M. Eldesoky and A. A. Farag, Effect of Adsorption and Interactions of New Triazole-Thione-Schiff Bases on the Corrosion Rate of Carbon Steel in 1 M HCl Solution: Theoretical and Experimental Evaluation, *ACS Omega*, 2024, **9**(6), 6761–6772, DOI: 10.1021/acsomega.3c08127.

4 A. Fawzy and A. Toghan, Inhibition evaluation of chromotrope dyes for the corrosion of mild steel in acidic environment: Thermodynamic and kinetic aspects, *ACS Omega*, 2021, **6**, 4051–4061.

5 H. M. Elabbasy, A. Toghan and H. S. Gadow, Cysteine as an Eco-Friendly Anticorrosion Inhibitor for Mild Steel in Various Acidic Solutions: Electrochemical, Adsorption, Surface Analysis, and Quantum Chemical Calculations, *ACS Omega*, 2024, **9**(11), 13391–13411, DOI: 10.1021/acsomega.3c10522.

6 A. Toghan, H. M. Dardeer, H. S. Gadow and H. M. Elabbasy, New promising halogenated cyclic imides derivatives as Potential Corrosion Inhibitors for Carbon Steel in Acidic Environment, *J. Molecular Liquids*, 2021, **325**, 115136–115156.

7 A. V. Polunin, A. P. Pschelnikov, V. V. Losev and I. K. Marshakov, Electrochemical studies of the kinetics and mechanism of brass dezincification, *Electrochim. Acta*, 1982, **27**, 467–475.

8 R. K. Dinnappa and S. M. Mayanna, The dezincification of brass and its inhibition in acidic chloride and sulphate solutions, *Corros. Sci.*, 1987, **27**, 349–361.

9 R. Trethewey and I. Pinwill, The dezincification of free-machining brasses in sea water, *Surf. Coat. Technol.*, 1987, **30**, 289–307.

10 J. Zou, D. Wang and W. Qiu, Solid-state diffusion during the selective dissolution of brass: Chronoamperometry and positron annihilation study, *Electrochim. Acta*, 1997, **42**, 1733–1737.

11 R. Karpagavalli and R. Balasubramaniam, Development of novel brasses to resist dezincification, *Corros. Sci.*, 2007, **49**, 963–979.

12 J. Morales, P. Esparza, S. Gonzales, L. Vasquez, R. C. Salvarezza and A. J. Arvia, Kinetics and mechanism of α-brass dealloying in aqueous 0.5 M sodium chloride solution derived from combined scanning tunneling microscopy and electrochemical data, *Langmuir*, 1996, **12**, 500–507.

13 H. Nady, Tricine[N-(Tri(hydroxymethyl)methyl)glycine]–A novel green inhibitor for the corrosion inhibition of zinc in neutral aerated sodium chloride solution, *Egypt. J. Pet.*, 2017, **26**, 905, DOI: 10.1016/j.ejpe.2016.02.004.
14 H. Martin, P. Carro, A. Hernandez Creus, J. Morales, G. Fernandez, P. Esparza, S. Gonzales, R. C. Salvarezza and A. J. Arvia, Inerplay of surface diffusion and surface tension in the evolution of solid/liquid interfaces. Dea loying of β-brass in aqueous sodium chloride, *J. Phys. Chem. B*, 2000, **104**, 8229–8237.
15 M. B. Valcarce, S. R. de Sanchez and M. Vazquez, Brass dezincification in a tap water bacterial suspension, *Electrochim. Acta*, 2006, **51**, 3736–3742; A comparative analysis of copper and brass surface films in contact with tap water. *J. Mater. Sci.* 2006, **41**, 1999–2007.
16 A. E. Warraky, Early stages of dezincification of α brass immersed in 4% NaCl solution, *Br. Corros. J.*, 1997, **32**, 57–62.
17 H. C. Shih and R. J. Tzou, Effect of benzotriazole on the stress corrosion cracking and the electrochemical polarization of 70/30 brass in fluoride solutions, *J. Electrochem. Soc.*, 1991, **138**, 958–961.
18 R. Nishimura and T. Yoshida, Stress corrosion cracking of Cu-30% Zn alloy in Mattsson's solutions at pH 7.0 and 10.0 using constant load method—A proposal of SCC mechanism, *Corros. Sci.*, 2008, **50**, 1205–1213.
19 A. Toghan, H. Alhussain, A. Attia, O. K. Alduaij, A. Fawzy, A. M. Eldesoky and A. Farag, Corrosion Inhibition Performance of Copper Using N-Benzylhy-Drazinecarbothioamide in a 3.5 % NaCl Solution: Original Scientific Paper, *J. Electrochem. Sci. Eng.*, 2024, **14**(2 SE-Corrosion), 231–245, DOI: 10.5599/jese.2181.
20 J. Morales, G. T. Fernandez, P. Esparza, S. Gonzalez, R. C. Salvarezza and A. J. Arvia, A comparative study on the passivation and localized corrosion of α, β, and α+β brass in borate buffer solutions containing sodium chloride—I. Electrochemical data, *Corros. Sci.*, 1995, **37**, 211–229.
21 J. Morales, P. Esparza, G. T. Fernandez, P. Esparza, S. Gonzalez, R. C. Salvarezza and A. J. Arvia, A comparative study on the passivation and localized corrosion of α-and β-brass in borate buffer solutions containing sodium chloride—II. X-ray photoelectron and Auger electron spectroscopy data, *Corros. Sci.*, 1995, **37**, 231–239.
22 A. M. Alfantazi, T. M. Ahmed and D. Tromans, Corrosion behavior of copper alloys in chloride media, *Mater. Des.*, 2009, **30**, 2425–2430.
23 M. Kabasakaloglu, T. Kıyak, O. Sendil and A. Asan, Electrochemical behavior of brass in 0.1 M NaCl, *Appl. Surf. Sci.*, 2002, **193**, 167–174.
24 K. M. Ismail, S. S. El-Egamy and M. Abdelfatah, Effects of Zn and Pb as alloying elements on the electrochemical behaviour of brass in borate solutions, *J. Appl. Electrochem.*, 2001, **31**, 663–670.
25 I. Milošev, T. K. Mikíč and M. Gaberščcek, The effect of Cu-rich sub-layer on the increased corrosion resistance of Cu–xZn alloys in chloride containing borate buffer, *Electrochim. Acta*, 2006, **52**, 415–426.
26 I. Milošev and T. Kosec, Electrochemical and spectroscopic study of benzotriazole films formed on copper, copper-zinc alloys and zinc in chloride solution, *Chem. Biochem. Eng. Q.*, 2009, **23**, 53–60.
27 R. Ravichandran, S. Nanjundan and N. Rajendran, Effect of benzotriazole derivatives on the corrosion and dezincification of brass in neutral chloride solution, *J. Appl. Electrochem.*, 2004, **34**, 1171–1176.
28 R. Ravinchandran, S. Nanjundan and N. Rajendran, Effect of benzotriazole derivatives on the corrosion of brass in NaCl solutions, *Appl. Surf. Sci.*, 2004, **236**, 241–250.
29 R. Ravinchandran and N. Rajendran, Influence of benzotriazole derivatives on the dezincification of 65–35 brass in sodium chloride, *Appl. Surf. Sci.*, 2005, **239**, 182–192.
30 T. Kosec, D. K. Merl and I. Milošev, Impedance and XPS study of benzotriazole films formed on copper, copper-zinc alloys and zinc in chloride solution, *Corros. Sci.*, 2008, **50**, 1987–1997.
31 T. Kosec, I. Milosev and B. Pihlar, Benzotriazole as an inhibitor of brass corrosion in chloride solution, *Appl. Surf. Sci.*, 2007, **253**, 8863–8887.
32 H. Gerengi, K. Darowicki, G. Bereket and P. Slepski, Evaluation of corrosion inhibition of brass-118 in artificial seawater by benzotriazole using dynamic EIS, *Corros. Sci.*, 2009, **51**, 2573–2579.
33 H. Gerengi and H. Bereket, Adsorption and inhibition effect of Benzotriazole on Brass-118 and Brass-MM55 in artificial seawater, *Prot. Met. Phys. Chem. Surf.*, 2012, **48**, 361–366.
34 H. Gerengi, K. Darowicki, P. Slepski, G. Bereket and J. Ryl, Investigation effect of benzotriazole on the corrosion of brassMM55 alloy in artificial seawater by dynamic EIS, *J. Solid State Electr.*, 2010, **14**, 897–902.
35 Z. Mountassir and A. Srhiri, Electrochemical behaviour of Cu-40Zn in 3% NaCl solution polluted by sulphides: Effect of aminotriazole, *Corros. Sci.*, 2007, **49**, 1350–1361.
36 J. R. Xavier, S. Nanjundan and N. Rajendran, Electrochemical adsorption properties and inhibition of brass corrosion in natural seawater by thiadiazole derivatives: experimental and theoretical investigation, *Ind. Eng. Chem. Res.*, 2012, **51**, 30–42.
37 M. Galai, K. Dahmani, M. EbnTouhami, R. Hsissou, F. Benhiba, M. Rbaa, M. Ouakki, R. Lachhab and S. M. Alharbi, Corrosion inhibition of brass electrode in 3% NaCl medium using novel quinoline derivatives based on D-glucose: Synthesis, characterization, and mechanistic insights through experimental and computational approaches, *Mater. Sci. Eng. B*, 2023, **298**, 116843.
38 M. G. K. Alfalah, A. E. Amgad, A. A. A. E. Kamberli, B. Nazlı, S. K. A. Tosun, M. Kad irlioğlu, F. Elkassum, S. Q. Saleh, A. Obıed and F. Kandemirli, Improvement of corrosion resistance for brass in 3.5% NaCl media by using 4-fluorophenyl-2, 5-dithiohydrazod icarbonamide, *J. Turk. Chem. Soc. A: Chem.*, 2023, **10**, 869–876.

39 G. Gao and C. H. Liang, 1,3-Bis-diethylamino-propan-2-ol as volatile corrosion inhibitor for brass, *Corros. Sci.*, 2007, **49**, 3479–3493.
40 M. B. Radovanović, M. B. Petrović, A. T. Simonović, S. M. Milić and M. M. Antonijević, Cysteine as a green corrosion inhibitor for Cu37Zn brass in neutral and weakly alkaline sulphate solutions, *Environ. Sci. Pollut Res Int*, 2013, **20**, 4370–4381.
41 H. Keles and S. Akca, The effect of Variamine Blue B on brass corrosion in NaCl solution, *Arab. J. Chem.*, 2019, **12**, 236–248.
42 R. Karpagavalli, R. Cairns Darran and S. Rajeswari, Synergistic inhibition effect of 2- mercaptobenzothiazole and Tween-80 on the corrosion of brass in NaCl solution, *Appl. Surf. Sci.*, 2008, **254**, 4483–4493.
43 H. Fan, S. Li, Z. Zhao, H. Wang, Z. Shi and L. Zhang, Inhibition of brass corrosion in sodi um chloride solutions by self-assembled silane films, *Corros. Sci.*, 2011, **53**, 4273–4281.
44 A. Nagiub and F. Mansfeld, Evaluation of corrosion inhibition of brass in chloride media using EIS and ENA, *Corros. Sci.*, 2001, **43**, 2147–2171.
45 M. B. Radovanović, Ž. Z. Tasić, M. B. Petrović Mihajlović, A. T. Simonović and M. M. Antonijević, Electrochemical and DFT studies of brass corrosion inhibition in 3% NaCl in the presence of environmentally friendly compounds, *Sci. Rep.*, 2019, **9**(1–16), 16081.
46 D. J. Karunarathne, A. Aminifazl, T. E. Abel, K. L. Quepons and T. D. Golden, Corrosion Inhibition Effect of Pyridine-2-Thiol for Brass in an Acidic Environment, *Molecules*, 2022, **27**(19), 6550.
47 E. M. Sherif and S. M. Park, Effects of 2-amino-5-ethylthio-1,3,4-thiadiazole on copper corrosion as a corrosion inhibitor in aerated acidic pickling solutions, *Electrochim. Acta*, 2006, **51**, 6556–6562.
48 S. L. F. A. De Costa, S. M. L. Agostinho and K. Nobe, Rotating ring-disk electrode studies of Cu-Zn alloy electrodissolution in 1 M HCl effect of benzotriazole, *J. Electrochem. Soc.*, 1993, **140**, 3483–3488.
49 N. Zulfareen, T. Venugopal and K. Kannan, Experimental and Theoretical Studies on the Corrosion Inhibition of Brass in Hydrochloric Acid by N-(4-((4-Benzhydryl Piperazin-1-yl) Methyl Carbamoyl) Phenyl) Furan-2-Carboxamide, *Int. J. Corr.*, 2018, **2018**, 372804.
50 D. Ozkir, E. Bayol, A. A. Gurten, Y. Surme and F. Kandemirli, Effect of hyamine on electrochemical behaviour of brass alloy in HNO_3 solution, *Chem. Pap.*, 2013, **67**, 202–212.
51 M. Ebrahimzadeha, M. Gholami, M. Momeni, A. Kosari, M. H. Moayeda and A. Davoodi, Theoretical and experimental investigations on corrosion control of 65Cu-35Zn brass in nitric acid by two thiophenolderivatives, *Appl. Surf. Sci.*, 2015, **332**, 384–392.
52 R. Selva Kumar and V. Chandrasekaran, Valoniopsis pachynema Extract as a Green Inhibitor for Corrosion of Brass in 0.1 N Phosphoric Acid Solution, *Metallurg. Mater. Trans. B*, 2016, **47**, 891–898.
53 M. M. Antonijevic, G. D. Bogdanovic, M. B. Radovanovic, M. B. Petrovic and A. T. Stamenkovic, Influence of pH and chloride ions on electrochemical behavior of brass in alkaline solution, *Int. J. Electrochem. Sci.*, 2009, **4**, 654–661.
54 S. K. Bag, S. B. Chakraborty, A. Roy and S. R. Chaudhuri, 2-Aminobenzimidazole as corrosion inhibitor for 70–30 brass in ammonia, *Br. Corros. J.*, 1996, **31**, 207–212.
55 V. Otieno-Alego, D. P. Schweinsberg, G. A. Hope and T. Notoya, An electrochemical and SERS study of the effect of 1-[N,N-bis-(hydroxyethyl)aminomethyl]-benzotriazole on the acid corrosion and dezincification of 60/40 brass, *Corros. Sci.*, 1996, **38**, 213–223.
56 X. J. Raj and N. Rajendran, Corrosion inhibition effect of substituted Thiadiazoles on Brass, *Int. J. Electrochem. Sci.*, 2011, **6**, 348–366.
57 T. Ramde, S. Rossi and C. Zanella, Inhibition of the Cu65/Zn35 brass corrosion by natural extract of *Camellia sinensis*, *Appl. Surf. Sci.*, 2014, **307**, 209–216.
58 T. Yanardag, S. Özbay, S. Dinçer and A. A. Aksüt, Corrosion inhibition efficiency of benzimidazole and benzimidazole derivatives for zinc, copper and brass, *Asian J. Chem.*, 2012, **24**, 47–52.
59 A. Fawzy, A. Al Bahir, N. Alqarni, A. Toghan, M. Khider, I. M. Ibrahim, H. H. Abulreesh and K. Elbanna, Evaluation of synthesized biosurfactants as promising corrosion inhibitors and alternative antibacterial and antidermatophytes agents, *Sci. Rep.*, 2023, **13**, 2585.
60 A. Toghan and A. Fawzy, Unraveling the adsorption mechanism and anti-corrosion functionality of dextrin and inulin as eco-friendly biopolymers for the corrosion of reinforced steel in 1.0 M HCl: A thermodynamic and kinetic approach, *Polymers*, 2023, **15**, 3144.
61 A. Fawzy, A. Toghan, N. Alqarni, M. Morad, M. E. A. Zaki, M. M. S. Sanad, A. I. Alakhras and A. A. Farag, Experimental and Computational Exploration of Chitin, Pectin, and Amylopectin Polymers as Efficient Eco-Friendly Corrosion Inhibitors for Mild Steel in an Acidic Environment: Kinetic, Thermodynamic, and Mechanistic Aspects, *Polymers*, 2023, **15**(891), 2170576, DOI: **10.3390/polym15040891**.
62 A. Toghan, A. Fawzy, N. Alqarni, A. Abdelkader and A. I. Alakhras, Inhibition effects of citrulline and glutamine for mild steel corrosion in sulfuric acid environment: Thermodynamic and kinetic aspects, *Int. J. Electrochem. Sci.*, 2021, **16**(1–21), 211118.
63 A. Fawzy, M. Abdallah, I. A. Zaafarany, S. A. Ahmed and I. I. Althagafi, Thermodynamic, kinetic and mechanistic approach to the corrosion inhibition of carbon steel by new synthesized amino acids-based surfactants as green inhibitors in neutral and alkaline aqueous media, *J. Mol. Liq.*, 2018, **265**, 276–291.
64 A. Toghan, A. Fawzy, A. I. Alakhras, N. Alqarni, M. E. A. Zaki, M. M. S. Sanad and A. A. Farag, Experimental Exploration, RSM Modeling, and DFT/MD Simulations of the Anticorrosion Performance of Naturally Occurring Amygdalin and Raffinose for Aluminum in NaOH

Solution, *Coatings*, 2023, **13**, 704, DOI: 10.3390/coatings13040704.

65 A. Fawzy, I. A. Zaafarany, H. M. Ali and M. Abdallah, New synthesized amino acids- based surfactants as efficient inhibitors for corrosion of mild steel in hydrochloric acid medium: kinetics and thermodynamic approach, *Int. J. Electrochem. Sci.*, 2018, **13**, 4575–4600.

66 A. Fawzy, R. El-Sayed, A. Al Bahir, M. Morad, I. Althagafi and K. Althagafy, Assessment of new designed surfactants as eco-friendly inhibitors for the corrosion of steel in acidic environment and evaluation of their biological and surface features: Thermodynamic, kinetic and mechanistic aspects, *J. Adh. Sci. Tech.*, 2022, 1997039.

67 A. Toghan, A. A. Alayyafi, H. Alhussain, M. E. A. Zaki, M. Khodari, N. Alqarni, E. M. Masoud, A. M. Eldesoky, A. A. Farag and A. Fawzy, Effect of Adsorption of Two Green Biopolymers on the Corrosion of Aluminum in 1.0 M NaCl Solution: Physicochemical, Spectroscopic, Surface and Quantum Chemical Exploration, *Int. J. Electrochem. Sci.*, 2024, **19**(10), 100791, DOI: 10.1016/j.ijoes.2024.100791.

68 A. Samide, G. E. Iacobescu, B. Tutunaru, R. Grecu, C. Tigae and C. Spînu, Inhibitory Properties of Neomycin Thin Film Formed on Carbon Steel in Sulfuric Acid Solution: Electrochemical and AFM Investigation, *Coatings*, 2017, **7**(11), 181.

69 A. Toghan, O. K. Alduaij, N. Alqarni, E. M. Masoud, H. Alhussain, A. M. Mostafa, A. A. Farag and A. Fawzy, Mathematical, Electrochemical, Spectroscopic and Microscopic Monitoring of the Adsorption Effect of Expired Drugs on Zinc Corrosion in 3.5% NaCl Solution. Results, *Chem*, 2025, **13**, 102006, DOI: 10.1016/j.rechem.2024.102006.

70 B. Anand and S. Chitra, Adsorption studies on the inhibition of the corrosion of mild steel in 2 M NaCl by tetracycline and neomycin trisulphate drugs, *Commun. Phys. Sci.*, 2020, **5**, 1–7.

71 M. Dehdab, Z. Yavari, M. Darijani and A. Bargahi, The inhibition of carbon-steel corrosion in seawater by streptomycin and tetracycline antibiotics: An experimental and theoretical study, *Desalination*, 2016, **400**, 7–17.

72 N. Alqarni, B. El-Gammal, A. Fawzy, A. Al Bahir and A. Toghan, Investigation of Expired Ticarcillin and Carbenicillin Drugs for Inhibition of Aluminum Corrosion in Hydrochloric Acid Solution, *Int. J. Electrochem. Sci.*, 2022, **17**, 2212113.

73 S. S. Medany, Y. H. Ahmad and A. M. Fekry, Experimental and theoretical studies for corrosion of molybdenum electrode using streptomycin drug in phosphoric acid medium, *Sci. Rep.*, 2023, **13**(1), 4827.

74 A. Toghan, O. K. Alduaij, A. Attia, A. Al Bahir, E. M. Masoud, H. M. Alhussain, A. Eldesoky, A. Farag and A. Fawzy, Exploring the Inhibitory Performance of Expired Moxifloxacin and Norfloxacin on Copper Corrosion in Saline Environment, *J. Electrochem. Sci. Eng.*, 2025, **15**(3), 2646, DOI: 10.5599/jese.2646.

75 S. Zehra; M. Mobin and J. Aslam Chapter 13—Chromates as corrosion inhibitors. In *Inorganic Anticorrosive Materials*, ed. Verma, C., Aslam, J. and Hussain, C. M., Elsevier, Amsterdam, The Netherlands, 2022, pp. 251–268.

76 G. Palanisamy, *Corrosion Inhibitors*, IntechOpen, London, UK, 2019.

77 A. Al-Amiery, W. N. R. W. Isahak and W. K. Al-Azzaw, Sustainable corrosion Inhibitors: A key step towards environmentally responsible corrosion control, *Ain Shams Eng. J.*, 2024, 102672, DOI: 10.1016/j.asej.2024.102672.

78 A. Fawzy, M. Abdallah and N. Alqarni, Kinetics and Mechanism of Oxidation of Neomycin and Streptomycin Antibiotics by Alkaline Permanganate, *Umm Al-Qura Univ. J. Appl. Sci.*, 2020, **6**(2), 1–5.

79 A. Toghan, A. A. Farag, O. K. Alduaij, H. M. Elabbasy, H. M. Dardeer, E. M. Masoud, A. Fawzy and H. S. Gadow, Electrochemical, Gravimetric, Quantum Chemical and Computational Investigations on an Effective Synthetic Chlorinated Cyclic Imide Derivative as a Corrosion Inhibitor for Carbon Steel in Sulfuric Acid Solution, *J. Mol. Struct.*, 2024, **1307**, 138040, DOI: 10.1016/j.molstruc.2024.138040.

80 A. A. Farag, A. A. Alayyafi, H. Alhussain, A. Fawzy, E. M. Masoud and A. Toghan, Corrosion Inhibition Performance of New Schiff Base Cyclohexanamine Derivatives on C-Steel in 1 M HCl Solution: Electrochemical, Chemical, Surface and Computational Explorations, *Inorg. Chem. Commun.*, 2024, **163**, 112339, DOI: 10.1016/j.inoche.2024.112339.

81 M. El Faydy, N. Timoudan, A. Barrahi, J. Bensalah, A. Thakur, A. A. Farag, B. Dikici, H. A. Abuelizz, B. Lakhrissi, A. Dafali and A. Zarrouk, Synthesis and Characterization of Two 8-Quinolinol Derivatives and Their Application as Corrosion Inhibitors for Carbon Steel in Hydrochloric Acid Solution, *J. Dispers. Sci. Technol.*, 2025, 1–17, DOI: 10.1080/01932691.2025.2557540.

82 M. El Faydy, N. Timoudan, A. Barrahi, A. A. Farag, A. Thakur, H. S. Kusuma, I. Warad, B. Lakhrissi, A. Dafali and A. Zarrouk, Inhibitory Performance of (E)-4-(3,4,5 Trimethoxyphenyl)but-3-En-2-One Crystal toward Carbon Steel Corrosion in Acid Medium by Practical and Theoretical Approaches, *J. Dispers. Sci. Technol.*, 2025, 1–16, DOI: 10.1080/01932691.2025.2462698.

83 N. S. Abdelshafi, A. A. Farag, A. A. M. Ali, A. A. Saleh, A. A. Zaher and R. Fouad, Multifunctional Novel Lanthanide Complexes Based on Chromone Moiety for Corrosion Inhibition, Molecular Docking, and Anticancer and Antimicrobial Applications, *Appl. Organomet. Chem.*, 2025, **39**(3), e70009, DOI: 10.1002/aoc.70009.

84 A. Fawzy, O. K. Alduaij, A. Al-Bahir, D. A. Alshammari, N. Alqarni, A. M. Eldesoky, A. A. Farag and A. Toghan, A Comparative Study of Pyridine and Pyrimidine Derivatives Based Formamidine for Copper Corrosion Inhibition in Nitric Acid: Experimental and Computational Exploration, *Int. J. Electrochem. Sci.*, 2024, **19**(1), 100403, DOI: 10.1016/j.ijoes.2023.100403.

85 A. A. Farag, S. M. Tawfik, A. A. Abd-Elaal and N. S. Abdelshafi, Detailed DFT/MD Simulation, QSAR Modeling, Electrochemical, and Surface Morphological Studies of Self-Assembled Surfactants as Eco-Friendly Corrosion Inhibitors for Copper in 1 M HNO3 Solution, *J. Ind. Eng. Chem.*, 2024, **138**, 237–255, DOI: 10.1016/j.jiec.2024.03.056.

86 T. H. A. Hasanina, A. M. Abd El Malak and S. A. M. Refaey, Corrosion Inhibition of Cu- Zn Alloys in NaCl Solution Using Isatin, Egypt, *J. Chem.*, 2021, **64**, 2377–2384.

87 A. Fawzy, A. Toghan, O. K. Alduaij, N. Alqarni, A. M. Eldesoky and A. A. Farag, Electrochemical, Spectroscopic, Kinetic and Surface Analysis of the Inhibitory Performance of Alcian Blue Dye for Copper Corrosion in Sulfuric Acid Solution, *Int. J. Electrochem. Sci.*, 2024, **19**(1), 100429, DOI: 10.1016/j.ijoes.2023.100429.

88 A. Toghan, H. Alhussain, A. Fawzy, M. M. S. Sanad, S. A. Al-Hussain, E. M. Masoud, H. Jiang and A. A. Farag, One-Pot Synthesis of N'-(Thiophen-2-Ylmethylene) Isonicotinohydrazide Schiff-Base as a Corrosion Inhibitor for C-Steel in 1 M HCl: Theoretical, Electrochemical, Adsorption and Spectroscopic Inspections, *J. Mol. Struct.*, 2024, **1318**, 139315, DOI: 10.1016/j.molstruc.2024.139315.

89 A. A. Farag, S. M. Elmesallamy, A. Bakry, D. S. Fathy, M. A. El-Etre and M. M. Badr, One-Pot Synthesis of Polybenzoxazine Resin *in Situ* Blended with Nano Extract Lawsonia Inermis as a Shield Coating for C-Steel in Acidic Environment: Experimental and Theoretical Approaches, *Ind. Crops Prod.*, 2025, **223**, 120306, DOI: 10.1016/j.indcrop.2024.120306.

90 A. A. Farag and A. Toghan, Unravelling the Adsorption and Anti-Corrosion Potency of Newly Synthesized Thiazole Schiff Bases on C-Steel in 1 M HCl: Computational and Experimental Implementations, *Results Eng*, 2025, **25**, 104504, DOI: 10.1016/j.rineng.2025.104504.

91 P. Manjula, S. Manonmani, P. Jayaram and S. Rajendran, Corrosion behaviour of carbon steel in the presence of N-cetyl-N, N, N-trimethylammonium bromide, Zn2+ and calcium gluconate, Anti-Corros, *Methods Mater.*, 2001, **48**, 319–324.

92 M. Erbil, The determination of corrosion rates by analysis of AC impedance diagrams, Chim, *Acta Turc*, 1988, **1**, 59–70.

93 F. Touhami, A. Aouniti, Y. Abed, B. Hammouti, S. Kertit, A. Ramdani and K. Elkacemi, Corrosion inhibition of armco iron in 1 M HCl media by new bipyrazolic derivatives, *Corros. Sci.*, 2000, **42**, 929–940.

94 X. Li, S. Deng, G. Mu, H. Fu and F. Yang, Inhibition effect of nonionic surfactant on the corrosion of cold rolled steel in hydrochloric acid, *Corros. Sci.*, 2008, **50**, 420–430.

95 M. Christov and A. Popova, Adsorption characteristics of corrosion inhibitors from corrosion rate measurements, *Corros. Sci.*, 2004, **46**, 1613–1620.

96 S. K. Shukla and M. A. Quraishi, Cefotaxime sodium: a new and efficient corrosion inhibitor for mild steel in hydrochloric acid solution, *Corros. Sci.*, 2009, **51**, 1007–1011.

97 T. K. Sarkar, M. Yadav and I. B. Obot, Mechanistic evaluation of adsorption and corrosion inhibition capabilities of novel indoline compounds for oil well/tubing steel in 15% HCl, *Chem. Eng. J.*, 2022, **431**, 133481.

98 M. Behpour, S. M. Ghoreishi, N. Soltani, M. Salavati-Niasari, M. Hamadanian and A. Gandomi, Electrochemical and theoretical investigation on the corrosion inhibition of mild steel by thiosalicylaldehyde derivatives in hydrochloric acid solution, *Corros. Sci.*, 2008, **50**, 2172–2181.

99 A. A. Farag, Oil-in-Water Emulsion of a Heterocyclic Adduct as a Novel Inhibitor of API X52 Steel Corrosion in Acidic Solution, *Corros. Rev.*, 2018, **36**(6), 575–588, DOI: 10.1515/corrrev-2018-0002.

100 A. A. Farag and M. A. Hegazy, Synergistic Inhibition Effect of Potassium Iodide and Novel Schiff Bases on X65 Steel Corrosion in 0.5M H2SO4, *Corros. Sci.*, 2013, **74**, 168–177, DOI: 10.1016/j.corsci.2013.04.039.

101 M. A. El-Monem, A. A. Farag, M. M. H. Khalil and M. A. Migahed, Hydroxyethyl Cationic Surfactants as Corrosion Inhibitors for S90 Steel in Produced Water: Electrochemical, and Computational Studies, *J. Mol. Struct.*, 2024, **1314**, 138702, DOI: 10.1016/j.molstruc.2024.138702.

102 A. A. Farag, S. M. Al-Shomar and N. S. Abdelshafi, Eco-Friendly Modified Chitosan as Corrosion Inhibitor for Carbon Steel in Acidic Medium: Experimental and in-Depth Theoretical Approaches, *Int. J. Biol. Macromol.*, 2024, 135408, DOI: 10.1016/j.ijbiomac.2024.135408.

103 S. M. Al-Shomar, A. Farag, F. Hedhili, H. S. Albaqawi, N. A. Al-Shammari, K. M. Abdel-Azim and N. S. Abdelshafi, Aminopyridine Schiff Bases as Eco-Friendly Corrosion Inhibitors for Carbon Steel in Acidic Media: Experimental and Quantum Chemical Insights, *J. Electrochem. Sci. Eng.*, 2025, **15**(4), 2769, DOI: 10.5599/jese.2769.

104 F. El-Dossoki, S. Abedelhady, M. Abedalhmeed, M. Abdel-Raouf and A. Ali, Micellization Properties, Molal Volume and Polarizability of Newly Synthesized Gemini-Cationic Surfactants. Egypt, *J. Chem.*, 2022, **65**, 585–599, DOI: 10.21608/ejchem.2021.71993.4507.

105 J. O. M. Bockris and A. K. N. Reddy, *Modern Electrochemistry*, vol. 2, Plenum Press, New York, 1977.

106 J. Marsh, *Advanced Organic Chemistry*, Wiley, Eastern New Delhi, 3rd edn, 1988.

107 S. A. A. El-Maksoud, F. I. El-Dossoki, M. Abd-Elhamed and A. A. Farag, Some New Synthesized Gemini Cationic Surfactants as Corrosion Inhibitors for Carbon Steel in Hydrochloric Acid Solution, *J. Bio- Tribo-Corrosion*, 2023, **9**(4), 71, DOI: 10.1007/s40735-023-00787-0.

108 M. A. Migahed; A. A. Farag; S. M. Elsaed; R. Kamal and H. Abd El-Bary Corrosion Inhibition of Carbon Steel in Formation Water of Oil Wells by Some Schiff Base Non Ionic Surfactants. In *European Corrosion Congress 2009 (EUROCORR 2009); Centre Francais de l'Anticorrosion (CEFRACOR)*: Nice, France, 2009; p. 871.

109 A. A. Farag, A. Toghan, M. S. Mostafa, C. Lan and G. Ge, Environmental Remediation through Catalytic Inhibition of Steel Corrosion by Schiff's Bases: Electrochemical and Biological Aspects, *Catalysts*, 2022, **12**(8), 838, DOI: 10.3390/catal12080838.

110 P. Singh, V. Srivastava and M. A. Quraishi, Novel quinolone derivatives as green corrosion inhibitors for mild steel in acidic medium: electrochemical, SEM, AFM, and XPS studies, *J. Mol. Liq.*, 2016, **216**, 164–173.

111 A. Toghan, A. Fawzy, A. I. Alakhras and A. A. Farag, Electrochemical and Theoretical Examination of Some Imine Compounds as Corrosion Inhibitors for Carbon Steel in Oil Wells Formation Water, *Int. J. Electrochem. Sci.*, 2022, **17**(12), 2212108, DOI: 10.20964/2022.12.94.

112 A. Toghan, A. Fawzy, A. G. Al-Gamal and A. A. Farag, Assessing the Inhibition Performance of Newly Synthesized Acridine-Pyrazole Derivatives on the Corrosion of Carbon Steel in HCl Solution: Experimental and Theoretical Approach, *J. Mol. Struct.*, 2025, **1345**, 143061, DOI: 10.1016/j.molstruc.2025.143061; N. S. Abdelshafi, A. A. Farag, F. E.-T. Heakal, A.-S. Badran, K. M. Abdel-Azim, A.-R. Manar El Sayed and M. A. Ibrahim, In-Depth Experimental Assessment of Two New Aminocoumarin Derivatives as Corrosion Inhibitors for Carbon Steel in HCl Media Combined with AFM, SEM/EDX, Contact Angle, and DFT/MDs Simulations, *J. Mol. Struct.*, 2024, **1304**, 137 638, DOI: 10.1016/j.molstruc.2024.137638.

113 A. Toghan, M. Khairy, M. Huang and A. A. Farag, Electrochemical, Chemical and Theoretical Exploration of the Corrosion Inhibition of Carbon Steel with New Imidazole-Carboxamide Derivatives in an Acidic Environment, *Int. J. Electrochem. Sci.*, 2023, **18**(3), 100072, DOI: 10.1016/j.ijoes.2023.100072.

114 E. A. Mohamed, A. A. Altalhi, A. Amer, N. A. Negm, E. A. M. Azmy and A. A. Farag, Two Novel Schiff Bases Derived from 3-Amino-1,2,4-Triazole as Corrosion Inhibitors for Carbon Steel Pipelines during Acidizing Treatment of Oil Wells: Laboratory and Theoretical Studies, *Energy Sources, Part A Recover. Util. Environ. Eff.*, 2023, **45**(2), 3246–3265, DOI: 10.1080/15567036.2023.2195817.

115 Y. Qiang, S. Zhang, S. Xu and W. Li, Experimental and theoretical studies on the corrosion inhibition of copper by two indazole derivatives in 3.0% NaCl solution, *J. Colloid Interface Sci.*, 2016, **472**, 52–59.

116 A. A. Farag and E. A. Badr, Non-Ionic Surfactant Loaded on Gel Capsules to Protect Downhole Tubes from Produced Water in Acidizing Oil Wells, *Corros. Rev.*, 2020, **38**(2), 151–164, DOI: 10.1515/corrrev-2019-0030.

117 Y. Qiang, S. Zhang and L. Wang, Understanding the adsorption and anticorrosive mechanism of DNA inhibitor for copper in sulfuric acid, *Appl. Surf. Sci.*, 2019, **492**, 228–238.

118 A. H, A. A. Mohamed and B. M. , B. Farag, Corrosion Inhibitiob of Mild Steel Using Emulsified Thiazole Adduct in Different Binder Systems, *Eurasian Chem. J.*, 2008, **10**(1), 67–77.

119 A. G. Al-Gamal, A. A. Farag, E. M. Elnaggar and K. I. Kabel, Comparative Impact of Doping Nano-Conducting Polymer with Carbon and Carbon Oxide Composites in Alkyd Binder as Anti-Corrosive Coatings, *Compos. Interfaces*, 2018, **25**(11), 959–980, DOI: 10.1080/09276440.2018.1450578.

120 L. H. Madkour, S. Kaya and I. B. Obot, Computational, Monte Carlo simulation and experimental studies of some arylazotriazoles (AATR) and their copper complexes in corrosion inhibition process, *J. Mol. Liq.*, 2018, **260**, 351–374.

121 M. S. Selim, A. N. El-hoshoudy, E. G. Zaki, A. M. EL-Saeed and A. A. Farag, Durable Graphene-Based Alkyd Nanocomposites for Surface Coating Applications, *Environ. Sci. Pollut. Res.*, 2024, **31**(31), 43476–43491, DOI: 10.1007/s11356-024-33339-1.

122 A. A. Farag and A. Toghan Recent Trends of Aqueous Phase Polymers as Corrosion Inhibitors for Various Metals in Harsh Environmental Conditions. In *Polymers as Corrosion Inhibitors*, Royal Society of Chemistry, 2025, pp. 91–103. DOI: 10.1039/9781837677214-00091.

123 Y. Qiang, S. Zhang, L. Guo, X. Zheng, B. Xiang and S. Chen, Experimental and theoretical studies of four allyl imidazolium-based ionic liquids as green inhibitors for copper corrosion in sulfuric acid, *Corros. Sci.*, 2017, **119**, 68–78.

124 N. S. Abdelsha, Electrochemical and molecular dynamic investigation of some new Pyrimidine derivatives as corrosion inhibitors for aluminium in acid medium, *Protection of Metals and Physical Chemistry of Surfaces*, 2020, **56**(5), 1066–1080, DOI: 10.1134/S2070205120050044.

125 Z. Amrani, A. Barrahi, A. A. Farag, A. Thakur, M. El Faydy, G. Kaichouh, Z. Safi, N. Wazzan, I. Warad and A. Zarrouk, Electrochemical, Theoretical, and Surface Characterization of Bis-Schiff-Based Corrosion Inhibitors on Carbon Steel in HCl Medium, *Colloids Surfaces A Physicochem. Eng. Asp.*, 2025, **709**, 136079, DOI: 10.1016/j.colsurfa.2024.136079.

126 K. F. Khaled, Studies of the corrosion inhibition of copper in sodium chloride solutions using chemical and electrochemical measurements, *Mater. Chem. Phys.*, 2011, **125**, 427–433.

127 E.-S. M. Sherif, Inhibition of Copper Corrosion Reactions in Neutral and Acidic Chloride Solutions by 5-ethyl-1,3,4-Thiadiazol-2-Amine as a Corrosion Inhibitor, *Int. J. Electrochem. Sci.*, 2012, **7**, 2832–2845.

128 P. Song, X.-Y. Guo, Y.-C. Pan, S. Shen, Y. Sun, Y. Wen and H.-F. Yang, Insight in cysteamine adsorption behaviors on the copper surface by electrochemistry and Raman spectroscopy, *Electrochim. Acta*, 2013, **89**, 503–509.

129 H. Shalaby, F. Al-Kharafi and V. Gouda, A Morphological Study of Pitting Corrosion of Copper in Soft Tap Water, *Corrosion*, 1989, **45**, 536.

130 A. L. Bacarella and J. C. Griess, The anodic dissolution of copper in flowing sodium chloride solutions between 25° and 175°C, *J. Electrochem. Soc.*, 1973, **120**, 459–465.
131 F. K. Crundwell, The anodic dissolution of copper in hydrochloric acid solutions, *Electrochim. Acta*, 1992, **37**, 2707–2714.
132 M. Scendo, The influence of adenine on corrosion of copper in chloride solutions, *Corros. Sci.*, 2008, **50**, 2070–2077.
133 A. A. Farag, A. S. Ismail and M. A. Migahed, Squid By-Product Gelatin Polymer as an Eco-Friendly Corrosion Inhibitor for Carbon Steel in 0.5 M H2SO4 Solution: Experimental, Theoretical, and Monte Carlo Simulation Studies, *J. Bio- Tribo-Corrosion*, 2019, **6**(1), 16, DOI: **10.1007/s40735-019-0310**.
134 H. Otmačić and E. Stupnišek-Lisac, Copper corrosion inhibitors in near neutral media, *Electrochim. Acta*, 2003, **48**, 985–991; G. Kear, B. D. Barker and F. C. Walsh, Electrochemical corrosion of unalloyed copper in chloride media – A critical review, *Corros. Sci.*, 2004, **46**, 109–135.